

Improving Accuracy Without Losing Interpretability: A Machine Learning Approach for Time Series Forecasting

Yiqi Sun

Department of Industrial Engineering, Tsinghua University, Beijing, China

Zhengxin Shi, Jianshen Zhang, Yongzhi Qi, Hao Hu

Intelligent Smart Y, JD.com, Beijing, China

Zuojun Max Shen

College of Engineering, University of California, Berkeley, Berkeley, California, USA

In time series forecasting, decomposition-based algorithms break aggregate data into meaningful components and are therefore appreciated for their particular advantages in interpretability. Recent algorithms often combine machine learning (hereafter ML) methodology with decomposition to improve prediction accuracy. However, incorporating ML is generally considered to sacrifice interpretability inevitably. In addition, existing hybrid algorithms usually rely on theoretical models with statistical assumptions and focus only on the accuracy of aggregate predictions, and thus suffer from accuracy problems, especially in component estimates. In response to the above issues, this research explores the possibility of improving accuracy without losing interpretability in time series forecasting. We first quantitatively define interpretability for data-driven forecasts and systematically review the existing forecasting algorithms from the perspective of interpretability. Accordingly, we propose the W-R algorithm, a hybrid algorithm that combines decomposition and ML from a novel perspective. Specifically, the W-R algorithm replaces the standard additive combination function with a weighted variant and uses ML to modify the estimates of all components simultaneously. We mathematically analyze the theoretical basis of the algorithm and validate its performance through extensive numerical experiments. In general, the W-R algorithm outperforms all decomposition-based and ML benchmarks. Based on P50_QL, a common evaluation indicator for quantile prediction, the algorithm relatively improves by 8.76% in accuracy on the practical sales forecasts of JD.com and 77.99% on a public dataset of electricity loads. This research offers an innovative perspective to combine the statistical and ML algorithms, and JD.com has implemented the W-R algorithm to make accurate sales predictions and guide its marketing activities.

Key words: time series forecasting, time series decomposition, machine learning, interpretability

1. Introduction

An algorithm with high accuracy, interpretability, and ability to deal with complex empirical data is the ultimate goal of forecasting. In time series forecasting, researchers have developed various approaches for different scenarios with distinct superiorities. Classical statistical methods, such as exponential smoothing (ETS for short) and autoregressive integrated moving average (ARIMA for short) models, have clear mathematical structure but can only handle simple time series data (De Gooijer and Hyndman 2006). These algorithms cannot capture the influence of exogenous variables and are, therefore, not satisfactory in accuracy, especially for non-stationary time series. The subsequent algorithms split into two main streams. One stream retains the statistical structure, focuses more on interpretability, and plays a crucial role in the industry. Typical examples are the state-space models that simplify the variation of time series through a discrete-time stochastic model (Sastri 1985, Snyder et al. 2017), and decomposition-based methods that split the aggregated data into interpretable components (Hyndman and Athanasopoulos 2021), such as the STL and Prophet algorithms (Cleveland et al. 1990, Taylor and Letham 2018). These algorithms either introduce the exogenous variables structurally or complicate the computational procedure for a better fit, but the improvement in prediction accuracy is limited. On the other hand, another stream prefers extreme prediction accuracy through black-box ML models. Related algorithms pay more attention to the efficient use of extensive empirical data and nonlinear relationships between the data and predictions. The majority of this stream is the neural networks (hereafter NN), such as Support Vector Machines (e.g., Kim 2003), Long-Short Term Memories (Hochreiter and Schmidhuber 1997), and Gate Recurrent Units (Cho et al. 2014). Nevertheless, the lack of interpretability has become a critical obstacle for these algorithms in practice (Molnar 2022).

Researchers have turned to hybrid algorithms that combine classical statistical models with black-box ML algorithms to improve forecasting accuracy and data processing ability. Most studies, including ours, focus on time series decomposition for its specific advantages in interpretability and flexibility. Additionally, proper decomposition extracts underlying patterns from aggregate panel data (Hyndman and Athanasopoulos 2021) and provides valuable insights for operations and supply chain management (Dokumentov and Hyndman 2022). Based on the popular Prophet algorithm, Triebe et al. (2021) proposes NeuralProphet, which uses statistical methods to predict the trend and seasonality components and NN for the auto-regression and exogenous effects. Following the statistical decomposition procedure, both Prophet and NeuralProphet predict the individual components through independent modules. In contrast, the N-BEATS and NBEATSx algorithms go further and deviate significantly from the traditional statistical approaches. Compared to the

NeuralProphet, these algorithms output the estimated components simultaneously through a connected NN consisting of different modules for the corresponding components and an additional module to predict the residuals between the simple addition and target value (Oreshkin et al. 2019, Olivares et al. 2022). For interpretability considerations, these algorithms, including the classic and hybrid methods, usually generate the final aggregate prediction by simply adding the components.

While claimed with multiple benefits, several remaining problems seriously restrict the further development of hybrid algorithms. First, the contradiction between interpretability and accuracy is likely inevitable (Murdoch et al. 2019). Therefore, with improved accuracy, hybrid algorithms are usually considered less interpretable after incorporating ML. We attribute this perception to the lack of quantification in the existing definition framework. To our knowledge, the existing definitions of ML interpretability are all ambiguous and abstract, such as those in Miller (2019), Murdoch et al. (2019), and Molnar (2022). In the absence of a well-defined concept, comparing the algorithms in interpretability usually relies on the model complexity (Zhou et al. 2018), which is improper in many cases. For example, the tree-based algorithms are often considered more interpretable than NN (e.g., in Guo et al. 2022). However, when the depth of trees reaches a milestone, such as a hundred, the relative advantage in interpretability becomes negligible. A more intuitive example is that a feed-forward NN with a single layer of 64 units is considered less interpretable than that of 32 units; however, they are about the same as people understand neither.

Moreover, the hybrid algorithms also succeed to the drawbacks of classical structural algorithms, which limit the further improvement in accuracy. In time series decomposition, the components are often generated through individual modules, and the final predictions are the simple addition of component estimates. These settings fail to capture the correlations among components and imply an assumption of independence. While it holds in some cases, the independence essentially relies on the components' mathematical definitions. For example, the trend and seasonality components are independent of each other as they respectively refer to the stable and periodic constituents of the time series. Accordingly, the ML modules have to strictly follow the structure of corresponding theoretical models, which restricts the potential for accuracy and efficiency. Worse yet, other components may be closely correlated, such as the impacts of promotion and advertising on sales. The forecasting models' performance would be compromised when the assumption of independence is not satisfied, which is likely to occur in reality.

In addition to the mandatory assumptions restricting the overall performance, there is a remaining issue for all decomposition-based algorithms: the less accurate prediction of components. As

only aggregate data are available, isolating the effects of various factors is tricky, and decomposition quality is difficult to examine. The measures breaking the components in existing algorithms usually rely on manual settings. For example, the parameters dividing the trend and seasonality components, which are supposed to change as appropriate automatically, are often pre-determined manually (e.g., in Cleveland et al. 1990, Dokumentov and Hyndman 2022). For the influence of exogenous variables, the estimates are usually simple linear impacts that are incomplete (e.g., in Triebe et al. 2021, Olivares et al. 2022). These problems lead to inaccurate component predictions, negatively affecting the total prediction accuracy and challenging the value of induced insights from proper decomposition.

To summarize, we focus on the following problems in this study and propose corresponding solutions.

1. *How to properly define interpretability in a quantitative manner?*

As noted before, a proper definition of interpretability is critical to the further development of hybrid algorithms. In this work, we propose an innovative definition of interpretability for data-driven forecasts, which divides the general concept into input and function interpretability. The novel definition allows us to compare the interpretability among algorithms quantitatively. Accordingly, we systematically review the existing algorithms from the perspective of interpretability, which reveals the possibility of improving accuracy without losing interpretability.

2. *Based on the quantitative definition of interpretability, how to improve the accuracy of the decomposition-based algorithms without losing interpretability?*

Inspired by the innovative definition of interpretability, we propose the W-R algorithm, which utilizes a weighted function to combine the components. Specifically, in the W-R algorithm,

$$Final\ Prediction = \sum_i (Weight \times Preliminary\ Prediction\ of\ Component\ i) + Residual,$$

where the weights and residuals are given by ML modules automatically. Note that the weighted combination function is equivalent to simple addition in interpretability as the parts multiplying weights can be considered as new estimates of components. We validate the advantages of the W-R algorithm through theoretical analysis and extensive numerical experiments.

3. *How to improve the prediction accuracy of components only with aggregate data?*

In addition to the overall performance, we are also curious about the forecasting accuracy of components, which is inherently tricky to analyze. Therefore, we first focus on a specific case with two components and derive the mathematical solutions and properties. For the special case, we derive conditions for both components to improve under the weighted mechanism, finding that

the conditions are likely to hold when the weights are in a moderate interval around 1. We then promote the findings into conjectures for the more general case and validate them through numerical experiments. To our knowledge, we are the first to consider the accuracy of components inside time series decomposition from a practical perspective.

4. Is the conflict between interpretability and accuracy always inevitable?

Taking the solutions to previous research problems together, we believe that the conflict between interpretability and accuracy is not always inevitable as long as we consider interpretability from a more general perspective. In the W-R algorithm, we implement the weighted combination function, which is different in complexity from the simple addition, but of the same level from the perspective of human understanding. Therefore, the W-R algorithm improves multi-dimensional accuracy without loss of interpretability.

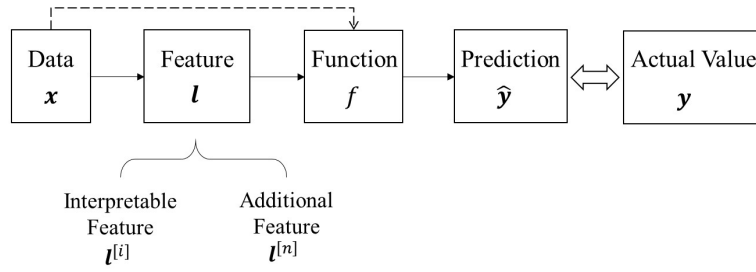
The remainder of the paper is organized as follows. In Section 2, we present the quantitative definition of interpretability and systematically review the related algorithms. Section 3 introduces the W-R algorithm with the weighted combination function, including theoretical analysis and concrete models for implementation. Section 4 reports the numerical results on the private and public datasets, and Section 5 concludes the paper. The E-companions (online supplements) present the mathematical proofs and the details for numerical experiments. In addition, we also provide background information on related algorithms for the convenience of readers.

2. Definition and Literature

2.1. Interpretability in Data-driven Forecasting

Let's start with a fundamental but persistent unanswered question: What is interpretability for forecasting algorithms? Existing definitions in literature are usually broad qualitative descriptions (Bertsimas et al. 2019, Molnar 2022). For example, Miller (2019) defines interpretability as the extent to which humans can understand the reasons for outputs from ML systems. And in Murdoch et al. (2019), interpretability refers to the ability to extract domain relationships contained in the data or learned by the model. Due to the stupefying complexity within, researchers have decomposed the concept from various perspectives for clarity. Du et al. (2020) differentiates ML interpretability into global and local interpretability, depending on whether one can understand all about the model or just a few results. Similarly, Molnar (2022) divides interpretable ML techniques into intrinsic interpretability, which arises from the ML algorithm itself, and post-hoc interpretability, which is model-agnostic and can be widely applied to all existing algorithms.

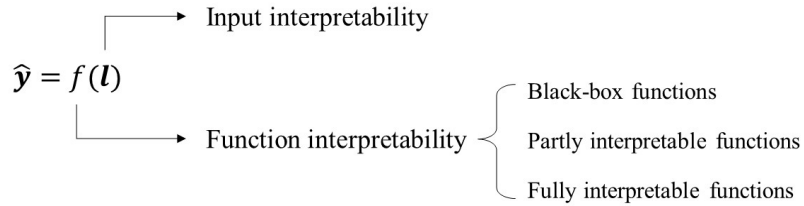
Figure 1 presents the general procedure of data-driven forecasting. There are four key elements inside, including the original data \mathbf{x} , the extracted features \mathbf{l} , the output prediction $\hat{\mathbf{y}}$, and the

Figure 1 The General Procedure of Data-driven Forecasting

function f capturing the relationship between the inputs and outputs. Note that the labels in bold represent vectors or matrices. While the model may include both the data and features as inputs in practice, we only consider the features as inputs, i.e.,

$$\hat{y} = f(l) \quad (1)$$

mathematically, as the data can be considered as features without any additional processing.

Figure 2 The Quantitative Definition Framework of Interpretability

According to Eq. (1), we divide the general interpretability of data-driven forecasting into the *input* and *function interpretability*, and illustrate the structure in Figure 2. The level of *input interpretability* refers to the relative proportion of interpretable features in inputs. Specifically, the interpretable features $l^{[i]}$ refer to those with specific meanings and can be understood by people directly, while other additional features $l^{[n]}$ only serve to improve the forecasting accuracy. In time series forecasting, typical interpretable features include the moving average features, such as the average sales in the past 7/14/28 days, and the features of exogenous variables, e.g., if there's a festival. Generally speaking, input interpretability is the basis of interpretable forecasting.

In contrast, *function interpretability* refers to the interpretability of function f , and is the primary deficiency for most less interpretable ML algorithms. From this perspective, we categorize the functions in existing algorithms into fully interpretable, partly interpretable, and black-box functions, denoted by f_i , f_p , and f_n , respectively. The fully interpretable functions have simple structural expressions that people can understand directly, such as linear regression and a single decision tree

with limited depth. Meanwhile, partly interpretable functions are those with complicated mathematical expressions that cannot be interpreted directly. Corresponding algorithms usually have identified rules for model generation, such as the random forests, the XGBoost, and other tree-based algorithms (see Breiman 2001, Chen and Guestrin 2016, for detail). In other words, people can directly understand the individual steps in these algorithms but not the aggregated outputs. Finally, the black-box functions refer to those that cannot be expressed by closed-form mathematics. The corresponding algorithms are usually not interpretable in both the generation procedure and output predictions. Representative examples in this category are the NN algorithms, including the popular Convolutional Neural Networks (CNNs), Recurrent Neural Networks (RNNs), and hundreds of variants. For the convenience of understanding, we list the key differences among these functions in Table 1.

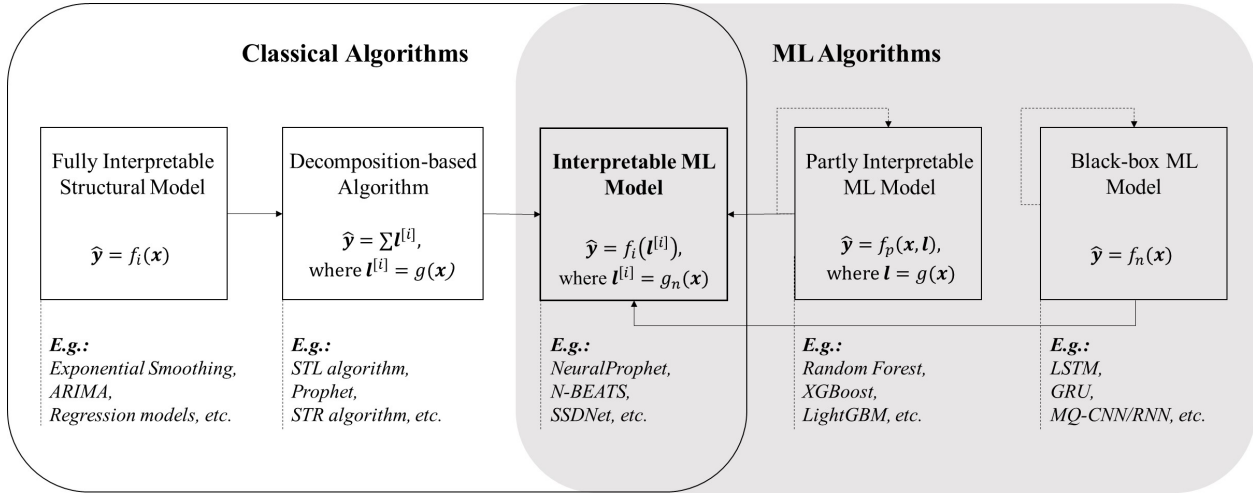
Table 1 Classifications of Functions in Interpretability

<i>Category of Functions</i>	For the function		For corresponding algorithm	
	Does the function have mathematical expression?	Does the mathematical expression simple enough to understand directly?	Can we separate the algorithm into interpretable steps?	Typical examples
<i>Fully interpretable</i>	Yes	Yes	Yes	Structural models
<i>Partly interpretable</i>	Yes	No	Yes	Rule-based algorithms
<i>Black-box</i>	No	No	No	Neural networks

In data-driven forecasting, an algorithm is interpretable if and only if the inputs and function are all interpretable. Mathematically, $\hat{\mathbf{y}} = f(\mathbf{l})$ is interpretable when $\mathbf{l} = \mathbf{l}^{[i]}$ and $f(\cdot) = f_i(\cdot)$. In other words, we should utilize ML modules to generate interpretable features and functions to improve accuracy without sacrificing interpretability. Note that our definition of interpretability mainly focuses on the interpretation of results rather than the detailed prediction procedures; therefore, there is still room for using black-box modules inside the algorithms. For example, as mentioned before, recent time series decomposition algorithms often utilize ML algorithms to predict the interpretable features (e.g., in Oreshkin et al. 2019, Triebe et al. 2021). The final outputs in these algorithms are the addition of the components, which is functionally interpretable.

2.2. Literature Review

We then systematically review the algorithms in time series forecasting from the perspective of interpretability. Figure 3 presents a unifying framework to classify related algorithms. There are mainly two streams of algorithms in data-driven forecasting, classical algorithms with high interpretability but low accuracy and ML algorithms that are exactly the opposite.

Figure 3 Classification Framework for Algorithms in Data-driven Forecasting

2.2.1. Classical Algorithms with Superior Interpretability As mentioned in Section 1, the early methods in time series forecasting are usually simple statistical/structural models with full interpretability. Typical examples include the ETS methods proposed by Holt (1957) and Winters (1960), ARIMA from Box and Jenkins (1970), and the historic regression models (e.g., Hyndman and Athanasopoulos 2021). These algorithms usually work directly on original time series data and have clear mathematical expressions for both the calculation procedure and output predictions. However, as we may expect, most of these algorithms cannot handle complex practical data and therefore are less satisfying in accuracy.

Subsequent researchers draw on the idea from Holt (1957) and Winters (1960) and generate a series of decomposition-based algorithms to improve forecasting accuracy. Up to now, related popular methods include the STL, Theta, Prophet, STR and STD algorithms for general time series (Cleveland et al. 1990, Assimakopoulos and Nikolopoulos 2000, Taylor and Letham 2018, Dokumentov and Hyndman 2022, Dudek 2022). In general, these algorithms first calculate the components through individual modules and then combine them additively (De Gooijer and Hyndman 2006, Hyndman and Athanasopoulos 2021). Common components consist of the trend, seasonality, and impacts of various exogenous variables (e.g., weather and holiday). Note that the components here are essentially equal to the features \mathbf{l} in Figure 1, and are likely to be interpretable to ensure the overall interpretability. Meanwhile, the modules calculating the components may be intricate to improve forecasting accuracy. For instance, the components in the STL algorithm, including the seasonality and trend, are generated by *Loess*, a weighted regression method based on the K-nearest-neighbor algorithm. In Prophet, the trend component is captured by a logistic growth model and a piecewise linear model, while the seasonality is described by the Fourier series.

Similar to the fully-interpretable structural models, the decomposition-based algorithms maintain distinctive superiority in interpretability and therefore play critical roles in forecasting practice (e.g., Snyder et al. 2017, Chuang et al. 2021). However, most methods are less efficient in processing the massive data generated by daily operations, resulting in accuracy issues. Moreover, as mentioned in Section 1, these algorithms usually rely on underlying assumptions, such as the pre-determined structure of components and the independence among components. These assumptions restrict the scope of application of the algorithms. Worse yet, the premises are likely to be broken in reality, making the performance less satisfying.

2.2.2. ML Algorithms with High Accuracy Contrary to classical methods, ML algorithms can handle complex data and are superior in accuracy but less satisfying in interpretability. A majority of the ML algorithms are the black-box NN algorithms, including the multilayer perceptron (MLP for short, e.g., Ahmed et al. 2010), CNN (e.g., Borovykh et al. 2019), RNN (see Hewamalage et al. 2021), and attention-based transformers (Vaswani et al. 2017). Note that while the transformers perform better in interpretability than CNN and RNN, the superiority is essentially not much from our perspective. The core of transformers is the self-attention function, which captures the self-interrelations of the outputs with a precise mathematical expression. However, the function generally serves as an intermediate step between other black-box modules in the application, making the whole algorithm less interpretable. Therefore, based on interpretability defined in Section 2.1, the pros and cons of attention-based algorithms are consistent with other NN models.

In time series forecasting, the popular NN models include the LSTM proposed by Hochreiter and Schmidhuber (1997), GRU from Cho et al. (2014), and TCN from Lea et al. (2016). Recent NN algorithms usually aim to meet specific requirements from practical applications, e.g., the WaveNet and DeepAR to predict quantiles (Oord et al. 2016, Salinas et al. 2020) and MQ-CNN/RNN for multiple quantile predictions with long forecasting horizon (Wen et al. 2017). These algorithms usually execute on normalized data and do not need additional assumptions on data or functions. However, while reported high accuracy, these algorithms are generally less interpretable and hence have problems in credibility, robustness, and troubleshooting (Molnar 2022).

Another category is the tree-based algorithms, with the highest interpretability among ML algorithms. Early tree methods only include a single decision tree, such as the classification and regression trees proposed by Breiman et al. (1984), therefore are fully interpretable when the number of nodes is limited. Later algorithms usually consist of several sub-trees for better robustness and accuracy, and the final output combines the outcomes from separate sub-trees. For example, the final prediction is the average of the sub-outputs in the random forest algorithm (Breiman

2001), and the addition in XGBoost and LightGBM (Chen and Guestrin 2016, Ke et al. 2017). As defined in Table 1, these algorithms are at least partly interpretable; However, as indicated in Murdoch et al. (2019), there is a common conflict between interpretability and predictive accuracy. In these tree models, a large number of features are often necessary to ensure predictive accuracy, which decreases input interpretability. Moreover, the massive features also inevitably increase the number of nodes and subtrees in the model, and the high complexity leads to low interpretability for the function f . In practice, the tree-based algorithms are likely to be partly interpretable to ensure forecasting accuracy, except for some straightforward cases when the model only needs a single decision tree with several nodes to achieve satisfying predictions.

To summarize, there are mainly two streams of ML algorithms in time series forecasting, the black-box NN and the tree-based algorithms with partial interpretability. Generally speaking, ML models with more input features and more sophisticated structures perform better in accuracy, implying a conflict between interpretability and accuracy. As people continue to pursue high accuracy, the deficiency of interpretability has become a critical concern for applying ML in practice.

2.2.3. Combination: Interpretable ML Model Researchers have integrated various methodologies to generate interpretable ML algorithms to simultaneously achieve nice accuracy and interpretability. These hybrid methods usually include two steps: (1) use ML to generate interpretable intermediate variables; (2) and then combine these intermediate outcomes through an interpretable function $f_i(\cdot)$. As indicated in Section 1, typical examples include the NeuralProphet, N-BEATS, NBEATSx, and SSDNet. The NeuralProphet algorithm proposed by Triaibe et al. (2021) succeeds to the structure of Prophet and generates the components through separate modules. Following Prophet, NeuralProphet uses statistical models in predicting the trend and seasonality but creatively utilizes NN to predict the effects of auto-regression and exogenous variables. Based on simple feed-forward NN, the N-BEATS algorithm proposed by Oreshkin et al. (2019) uses sequential NN modules to simultaneously predict the components of trend, seasonality, and residuals. Afterward, Olivares et al. (2022) considers the impacts of exogenous variables and extends N-BEATS to the NBEATSx. While the components are generated simultaneously, these two algorithms severely rely on the physical definitions of components. For specific components, the structure inside the corresponding module depends on the theoretical model, precisely, the polynomial regression for the trend and periodic functions (i.e., $\sin(\cdot)$ and $\cos(\cdot)$) for the seasonality part. Similarly, the SSDNet algorithm utilizes NN to simulate a state space model, another theoretical model capturing the time-related variations of the components (Lin et al. 2021). Consistent with

other algorithms mentioned above, the SSDNet also divides the time series into components of seasonality, trend, and random error, and the final prediction is the simple addition of the components for specific forecasting periods.

These algorithms have several common characteristics and hence similar problems. First, all of the interpretable ML algorithms mentioned above only incorporate ML in the prediction of components. As a result, the deficiencies of the classic decomposition algorithms still hold for these algorithms. The final predictions usually follow a simple additive form, i.e.,

$$\hat{y} = \sum_j l_j^{[i]} \quad (2)$$

where $l_j^{[i]}$ denotes the j th explainable component. The equation is simple with full interpretability; However, as discussed in Sections 1 and 2.2.1, without additional consideration on correlations, it implies the assumption of independence among components, and restricts the design of decomposition-based algorithms. Most algorithms only consider independent components, such as seasonality, trend, and residuals. The corresponding NN modules are designed following the deep logic of the theoretical models built on the mathematical definitions. Other components, such as the effects of exogenous variables in NeuralProphet and NBEATSx, are usually modeled by a simple linear function without cross-component interrelations. That is, the ML modules only serve as the agent of theoretical models. Therefore, the benefits of ML, especially the tolerance of statistical assumptions, are reduced, which limits the forecasting accuracy and further application in practice.

Finally, it is worth mentioning that the problem of lacking independence is magnified when we turn to the specific time series on sales. Compared with general time series, sales are significantly influenced by several exogenous factors, which have been indicated in extensive empirical and theoretical literature. Taking these elements into consideration would help improve forecasting accuracy. For example, in addition to the components of seasonality and trend, the SCAN*PRO algorithm integrates price, competition, and advertising (Wittink et al. 1988), and the CHAN4CAST method further incorporates past sales, temperature, and holiday (Divakar et al. 2005). However, these factors are nearly impossible to be entirely independent of other factors. For example, price discounts and advertising always occur concurrently for the same promotion activities, periodically or with intense competition. Meanwhile, the various influencing factors of a given seller may be highly consistent due to the same sales target or specific enterprise culture. In this case, the common additive combination function in existing algorithms is challenged from a fundamental perspective.

2.2.4. Summary To summarize, incorporating ML in decomposition-based time series forecasting has become an inevitable trend for simultaneous benefits in accuracy and interpretability. ML methods have natural superiority in dealing with massive practical data and capturing non-linear relationships without strict statistical assumptions. However, existing relevant algorithms only utilize ML in the separate forecast of components, and the inappropriate assumption of independence still holds in the additive form of total predictions. The improper assumption restricts the accuracy of predictions, especially those on the decomposed components.

In this research, we propose W-R Algorithm, a hybrid forecasting algorithm following the interpretable ML stream but focusing more on the combination function $f_i(\cdot)$, in addition to the prediction of components. Specifically, the combination function follows a weighted linear form, where the parameters are generated from ML modules. Therefore, it is still interpretable but more accurate than the simple additive function. This idea is essentially similar to the optimal tree method proposed by Bertsimas et al. (2021), which aims to improve a tree with proper design. However, our algorithm is built on a linear combination function rather than the trees; therefore, the decision spaces are of distinct forms. Moreover, while the optimal trees utilize mixed integer programming to determine the optimal splits, our algorithm uses ML to determine the improved parameters, proving efficient through theoretical analysis and numerical experiments.

3. The W-R Algorithm for Interpretable Forecasting

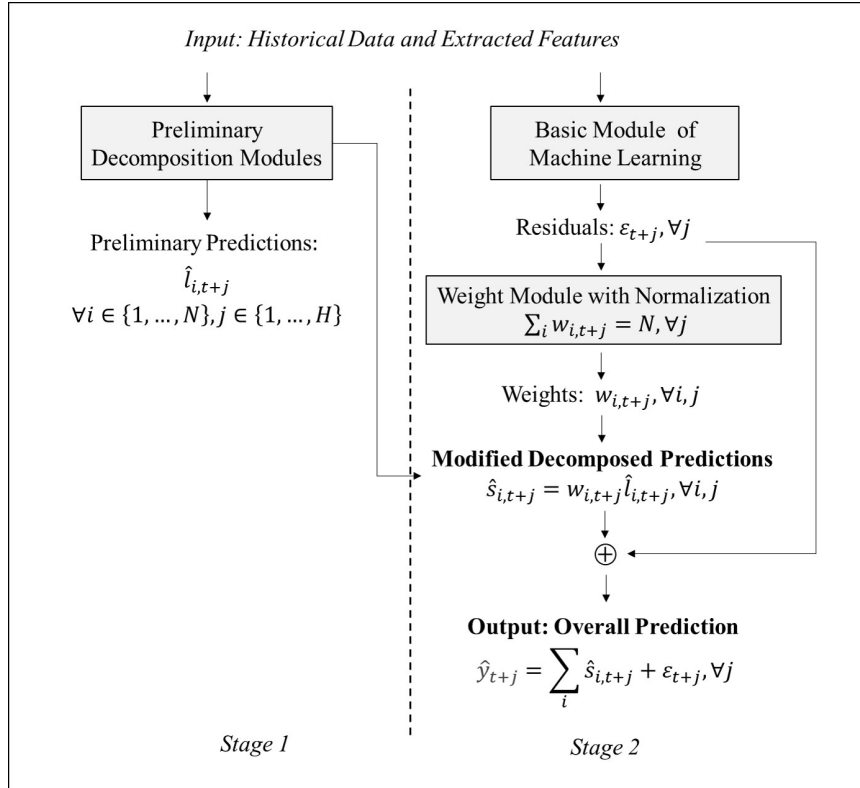
This section details the W-R algorithm with the weighted combination function. Section 3.1 first introduces the algorithm’s general structure, and Section 3.2 theoretically analyzes the weighted mechanism. Finally, in Section 3.3, we describe the implementation details of the W-R algorithm.

3.1. General Structure

Consistent with the recent algorithms for time series forecast (e.g., Wen et al. 2017, Lim et al. 2021), our algorithm predicts the quantiles in multiple forecasting horizon. Let N , t , and H respectively denote the number of components, time of forecasting, and forecasting horizon. Then the task is to predict the time series of the following H periods from time t , denoted by $\hat{\mathbf{y}} = \{\hat{y}_{t+j}, \forall j \in \{1, \dots, H\}\}$. The target is to minimize the difference between $\hat{\mathbf{y}}$ and the actual value \mathbf{y} .

As illustrated in Figure 4, the W-R algorithm includes two connected stages. Stage 1 generates the preliminary decomposition according to historical data and extracted features. Mathematically, the preliminary estimates of component i for period $t+j$ is denoted by $\hat{l}_{i,t+j}$, where $i \in \{1, \dots, N\}$, $j \in \{1, \dots, H\}$. The specific approaches of preliminary decomposition are flexible, depending on the practical scenario and characteristics of the data.

Figure 4 General Structure of the W-R algorithm



Most existing decomposition-related algorithms for time series forecasting only include the above stage, in which the final predictions are the simple addition of the components (e.g., Winters 1960, Cleveland et al. 1990, Taylor and Letham 2018). Through an additional ML module with a clear structure, the W-R algorithm further improves the preliminary estimates in stage 2. As highlighted in the algorithm's name, two key intermediate elements, \mathbf{w} and ε , serve as the weights and residuals in the weighted combination function to modify the naive predictions.

Specifically, in stage 2, the original data and features are first put into a basic ML module and generate an intermediate variable $\varepsilon = \{\varepsilon_{t+j}, \forall j \in \{1, \dots, H\}\}$. Compared with statistical methods, the ML algorithm better discovers the underlying non-linear relationship between the complex practical data and predictions. The intermediate output ε is then put into a weight module, of which the output is denoted by $\mathbf{w} = \{w_{i,t+j}, \forall i \in \{1, \dots, N\}, j \in \{1, \dots, H\}\}$. Constrained by $\sum_i w_{i,t+j} = N$, \mathbf{w} serves as the weight factor to modify the decomposed predictions, and the modified predictions on components are $\hat{s}_{i,t+j} = w_{i,t+j} \hat{l}_{i,t+j}, \forall i \in \{1, \dots, N\}, j \in \{1, \dots, H\}$. Finally, we merge the modified prediction with ε by the residual connection method (He et al. 2016), hence the overall prediction is $\hat{\mathbf{y}} = \{\hat{y}_{t+j} = \sum_i \hat{s}_{i,t+j} + \varepsilon_{t+j}, \forall i \in \{1, \dots, N\}, j \in \{1, \dots, H\}\}$. As it denotes the difference between \hat{y}_{t+j} and the weighted sum of components, and we call ε_{t+j} the *residual*.

The advantages of the W-R algorithm are manifold. First, the weighted combination function is a simple linear equation with full function interpretability. As a result, the algorithm is highly interpretable as long as the components are meaningful. Besides, the naive predictions on components are modified through the ML algorithm, hence are more accurate (we'll analyze this afterward) and valuable for subsequent analysis and decision-making. Moreover, through extensive numerical experiments, the W-R algorithm also performs better than the individual algorithms within, such as the basic ML module in stage 2. This phenomenon indicates the importance of domain knowledge; that is, information on proper decomposition would help model performance. Finally, the W-R algorithm owns excellent flexibility in application. We can select different methods for preliminary decomposition and the basic ML module within to meet various requirements in practice.

3.2. Theoretical Analysis on the Weight Mechanism

We then explore the underlying mechanism behind the W-R algorithm theoretically. The core of the algorithm is the weighted combination function, i.e.,

$$\hat{y}_{t+j} = \sum_{i=1}^N w_{i,t+j} \hat{l}_{i,t+j} + \varepsilon_{t+j} \quad \text{with} \quad \sum_i w_{i,t+j} = N. \quad (3)$$

Originating from simple linear regression, the weighted mechanism is quite common in theory and practice. In our case, we allocate different weight parameters for different preliminary estimations (i.e., $w_{i,t+j}$ for $\hat{l}_{i,t+j}$), therefore our weighted mechanism is *dynamic* rather than static as in regressions. This setting copes with the dynamic characteristics of estimation biases; that is, the estimation biases usually vary with different components and over time. As a result, the prediction accuracy would be better than the static model. Moreover, by adding weights to the individual components for distinct periods, the independence assumption is not required in our case. However, the incorporation of additional parameters significantly increases the dimension of the feasible region and the difficulty of solving. According to the following theoretical analysis, we take two measures in response.

As Eq. (3) works for all forecasting horizons, we omit the subscript $t+j$ in the rest of this subsection for simplicity. As we expected, the residual term ε helps improve the forecasting accuracy, as it accounts for the unconsidered components, such as the effects of some exogenous variables. As a result, we mainly want to discuss the effectiveness of the weight mechanism here, where the benchmark is the common additive function. Mathematically, the weighted combination function without residual is expressed as $\hat{y} = \sum_{i=1}^{N-1} w_i \hat{l}_i + (N - \sum_{i=1}^{N-1} w_i) l_N$, while the additive combination function is $\hat{y} = \sum_{i=1}^N \hat{l}_i$. The actual relationship behind is supposed to be $y = \sum_{i=1}^{N-1} l_i$, where l_i and l_j can be correlated with each other when $i \neq j$.

3.2.1. The Overwhelming Advantage in Overall Accuracy It is not surprising that the weighted combination shows absolute superiority in forecasting accuracy compared with the simple addition. For the convenience of mathematics, we first consider a special case with $N = 2$. We label the two components l_1 and l_2 , and the estimates are \hat{l}_1 and \hat{l}_2 , respectively. Then for the weighted combination function without residual, the prediction $\hat{y} = w\hat{l}_1 + (2 - w)\hat{l}_2$, with only 1 parameter w to optimize. We only consider the case with unequal components, as the prediction would stay constant when $\hat{l}_1 = \hat{l}_2$. Without loss of generality, we assume $\hat{l}_1 > \hat{l}_2$.

PROPOSITION 1. *When $N = 2$, there exists a unique weight parameter $w^* = \frac{y - 2\hat{l}_2}{\hat{l}_1 - \hat{l}_2}$ optimizing the weighted combination function without residual, and the weighted combination with optimized w^* never performs worse in accuracy than the simple addition. Specifically,*

1. *if $y = \hat{l}_1 + \hat{l}_2$, these two functions show equivalent accuracy;*
2. *Otherwise, if $y \neq \hat{l}_1 + \hat{l}_2$, the optimized weighted combination performs better.*

Proposition 1 indicates the superiority of the weight mechanism over the common additive function in the specific case. The principle behind it is quite simple, as the additive function is a special case of the weighted combination function, i.e., all weight parameters equal 1. A detailed proof is given in EC.1.1. Moreover, the weighted combination function performs better than the additive function unless the additive function already achieves the best. However, the performance of simple addition is usually far away from the optimum in practice.

PROPOSITION 2. *When $N > 2$, there exist infinite groups of the weight parameters optimizing the weighted combination function without residual. With optimized parameters, the optimized combination function performs better in accuracy than the simple addition as long as $y \neq \sum_i \hat{l}_i$.*

As shown in Proposition 2, the superiority of the weight mechanism stays valid for the case with more components. However, the large feasible region of $\{w_i, \forall i \in \{1, \dots, N\}\}$ reduces the underlying consistency of estimations. We take two measures to reduce the size of the feasible region. First, we incorporate the summing-up constraint $\sum_i w_i = N$ to reduce the dimension of the feasible region by 1. In addition, we restrict the feasible region of each weight parameter in the application, which is proved effective through extensive numerical experiments.

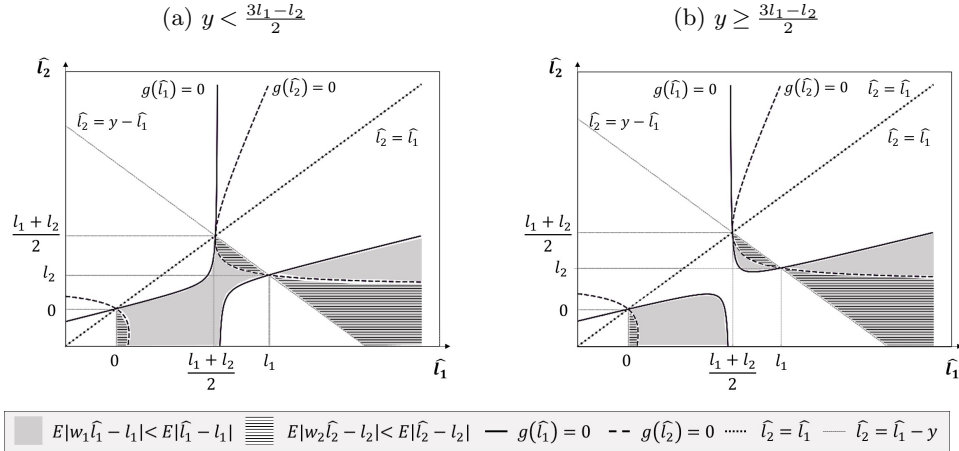
3.2.2. Impact on Prediction Biases of Components In addition to the overall forecasting accuracy, we are curious about the quality of modified prediction on the components. Specifically, remind that l_i and \hat{l}_i respectively denote the actual value and estimate of component i , and w_i is the corresponding weight parameter. Then we want to know that under which condition $|w_i\hat{l}_i - l_i| < |\hat{l}_i - l_i|$, i.e., the modified estimate is less biased than the original prediction. Similar to the analysis in Section 3.2.1, we start with the specific case with $N = 2$ for the convenience of mathematics.

PROPOSITION 3. When $N = 2$, let $-i$ label the other component of component i , and $g(\hat{l}_i) = \hat{l}_i^2 + \hat{l}_i(y - 3\hat{l}_{-i} - 2l_i) + 2l_i\hat{l}_{-i}$. Then we have:

1. When $y > \hat{l}_1 + \hat{l}_2$, the modified estimate with optimal weight $w_i^*\hat{l}_i$ is less biased than the original prediction \hat{l}_i if and only if $g(\hat{l}_i) < 0$;
2. Otherwise, when $y < \hat{l}_1 + \hat{l}_2$, $w_i^*\hat{l}_i$ is less biased than \hat{l}_i if and only if $g(\hat{l}_i) > 0$.

Proposition 3 shows the conditions of bias reduction for separate components when $N = 2$. The variation of biases for component relies on the relative relationship between y and $\hat{l}_1 + \hat{l}_2$ (i.e., the prediction with additive combination function), as well as a quadratic function $g(\hat{l}_i)$, which is strictly convex over \hat{l}_i . When the additive combination function under-estimates the actual value, i.e., $y > \hat{l}_1 + \hat{l}_2$, the component i is improved after multiplying w_i^* when $g(\hat{l}_i) < 0$. Otherwise, when $y < \hat{l}_1 + \hat{l}_2$, the additive combination over-estimates the actual value, and the component i is improved with w_i^* if and only if $g(\hat{l}_i) > 0$.

Figure 5 The Impact of Weight Mechanism on Prediction Biases of Components ($N = 2$)



We then explore the conditions for both components to improve with the optimized weights. However, $g(\hat{l}_i)$ and $g(\hat{l}_{-i})$ are two connected quadratic functions, making the joint inequities intricate to solve. Moreover, the mathematical expressions in Proposition 3 are messy, making the solutions for joint improvement difficult to interpret directly. Therefore, we illustrate the conditions in Figure 5, where the shaded region denotes the improvement of component 1, and the area with horizontal lines indicates reduced biases of constituent 2. The mathematical conditions for both components improve after the weight mechanism is given by Corollary 1, illustrated by the shaded area with horizontal lines in Figure 5. Consistent with Section 3.2.1, we assume $\hat{l}_1 > \hat{l}_2$ here.

COROLLARY 1. In the specific case with $N = 2$, suppose $\hat{l}_i > 0 \forall i = \{1, 2\}$. Then we have:

1. When $\frac{l_1+l_2}{2} < \hat{l}_1 < l_1$, there exists unique $l_{20}^* \in (l_2, \frac{l_1+l_2}{2})$ making $g(\hat{l}_2) = 0$, and both of the components improve after multiplying with the optimal weights if and only if $l_{20}^* < \hat{l}_2 < \hat{l}_1 - y$.
2. When $\hat{l}_1 > l_1$, there exists unique $l_{21}^* \in (0, l_2)$ making $g(\hat{l}_2) = 0$, and both of the components improve after multiplying with the optimal weights if and only if $\hat{l}_1 - y < \hat{l}_2 < l_{21}^*$.

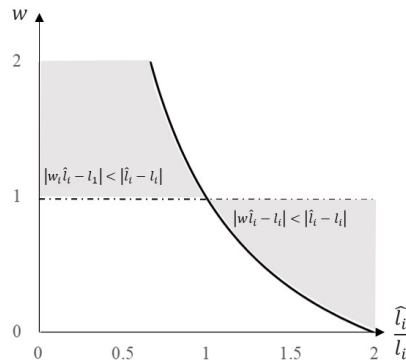
OBSERVATION 1. In the specific case with $N = 2$, suppose $\hat{l}_i > 0 \forall i = \{1, 2\}$, $\hat{l}_1 > \hat{l}_2$. Then when $\hat{l}_1 > \frac{l_1+l_2}{2}$, $w^* \in (0, 2)$. Specifically, when $\frac{l_1+l_2}{2} < \hat{l}_1 < l_1$, $w^* \in (1, 2)$; when $\hat{l}_1 > l_1$, $w^* \in (0, 1)$.

Generally speaking, there are two scenarios that both components improve, (1) when l_1 is over-estimated and l_2 is under-estimated, and the opposite, (2) when l_1 is under-estimated and l_2 is over-estimated. In both cases, the original biases for these components are opposite, and the absolute percentages of biases are comparable. Besides, the joint improvement of components is more likely to occur when the additive combination $\hat{l}_1 + \hat{l}_2$ is not far from the actual value y . This situation is essentially reasonable from the deep logic of the weighted mechanism, i.e., the redistribution function. On the contrary, if both components are over- or under-estimated, it is impossible to reduce the biases simultaneously. Under the optimized scenarios in Corollary 1, Observation 1 shows the feasible region of w^* when $N = 2$, which is quite intuitive. When both of the components are positive, w^* should be in $(0, 2)$ to ensure $w_i > 0, \forall i \in \{1, 2\}$.

PROPOSITION 4. For the general case with $\hat{l}_i > 0$, $|w_i \hat{l}_i - l_i| < |\hat{l}_i - l_i|$ if and only if:

1. $\hat{l}_i < l_i$, and $1 < w_i < \frac{2l_i}{\hat{l}_i} - 1$;
2. Or $\hat{l}_i > l_i$, and $\frac{2l_i}{\hat{l}_i} - 1 < w_i < 1$.

Figure 6 The Impact of Weights on Prediction Biases of Components ($\hat{l}_i > 0, l_i > 0$)



We finally turn to the general case when $N \geq 2$. Without loss of generality, we focus on the case of $\hat{l}_i > 0$ here. Proposition 4 presents the general condition for single component in this case, and the graphical illustration is given by Figure 6. Specifically, when the component is under-estimated (i.e., $\hat{l}_i < l_i$), the weight mechanism would reduce the forecasting bias when w_i is a bit larger than

1; and the case of over-estimated (i.e., $\hat{l}_i > l_i$) is just the opposite. The other threshold of w_i besides 1 is positively related to the relative size of l_i/\hat{l}_i . When $\hat{l}_i < l_i$ (or $\hat{l}_i > l_i$), the available region of w_i for reduced biases decreases (increases) with \hat{l}_i when l_i is fixed. When $\hat{l}_i = 0$, the weight mechanism does not work as the multiplication stays 0. And finally, if $\hat{l}_i < 0$ (which is less likely to happen), the results are opposite, and the details are given in Proposition EC.1 in EC.1.4.

CONJECTURE 1. *For the general case with N components and non-negative estimates, it is more likely to happen that the weight mechanism improves the estimation of all components when*

1. *y is relatively close to $\sum_j \hat{l}_j$,*
2. *and the optimal weights $w_i^* \forall i \in \{1, \dots, N\}$ are in a moderate interval around 1.*

Note that we can only give a general condition with w_i when N is not limited, as the optimal solutions are not unique. However, taking the results from the particular case of $N = 2$ and Proposition 4, we have Conjecture 1 for the general conditions of joint components improvement. It suggests that the estimations on components are more likely to improve by the weight mechanism when the weight parameters are close to 1. As the exact values of components are unavailable, we validate the conjecture through the overall accuracy in numerical experiments. Specifically, we restrict the feasible region of w_i to $[1 - \frac{\alpha}{N}, 1 + \alpha - \frac{\alpha}{N}]$, where $\alpha \in (0, N)$ is a manually determined parameter. Under Conjecture 1, the overall accuracy would be better when α is moderate, as the estimations on components should be more accurate.

3.2.3. Discussion To summarize, we theoretically analyze the impacts of the weight mechanism without residual on the overall accuracy and components' prediction errors. For the specific case of $N = 2$, we derive the unique solution of optimal weights and present the mathematical conditions to reduce the prediction errors of both components. However, for the more general case of $N > 2$, the weight parameters minimizing the overall prediction gap are infinite. Inspired by the special case, we guess the component estimates may be less biased when the optimal weights are in a moderate interval around 1. As the exact values of components are unavailable, we believe black-box ML rather than statistical methods would be more appropriate for calculating the weights. To reduce the difficulty of the calculation, we reduce the feasible region of weights by incorporating a summing-up constraint and forcing each weight within a certain range around 1.

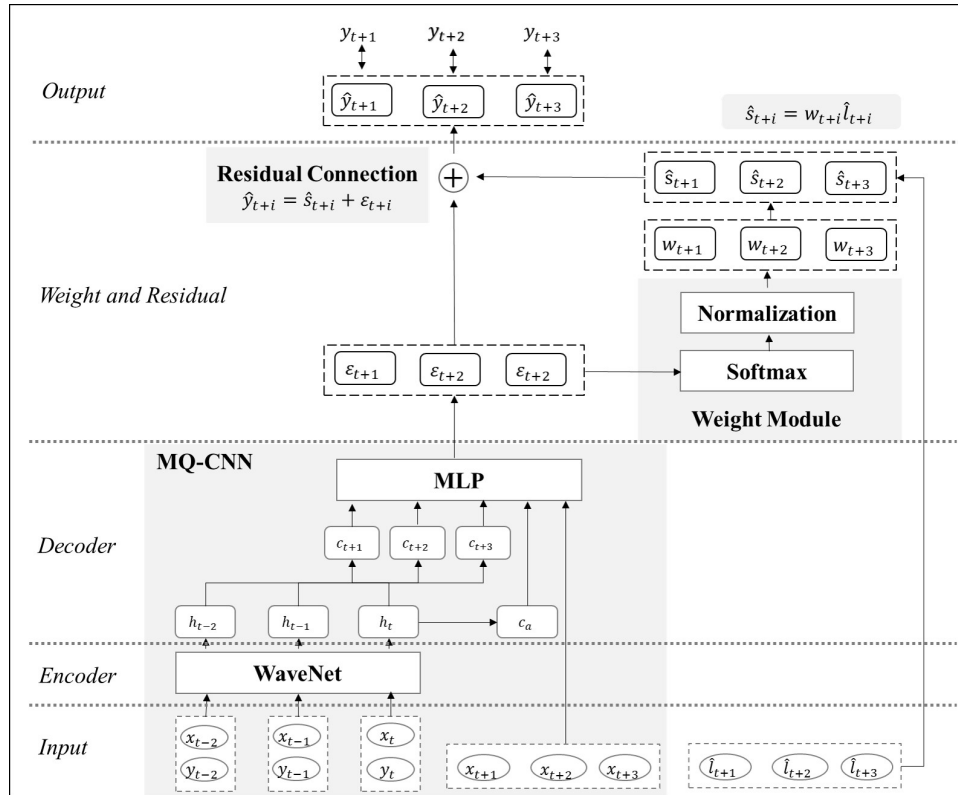
While we only analyze the weighted mechanism without residual here, the main results for the general case still hold for the case with residual. The only difference is replacing \hat{y} and y by $\hat{y} - \varepsilon$ and $y - \epsilon$, where ε and ϵ denote the estimate and actual value of the residual, respectively. The incorporation of residual would enlarge the feasible region of alternative parameters and hence

increase the calculation complexity. However, it also increases the possibility of bias reduction with improved accuracy, especially when the original prediction with the additive function $y_{additive}$ is less satisfying in accuracy.

3.3. Concrete Models for Implementation

We finally introduce the implementation details of the W-R algorithm in numerical experiments. Section 3.3.1 presents the MQ-CNN-based module for stage 2, which is committed to improving the forecasting accuracy through the weighted combination function. Sections 3.3.2 and 3.3.3 describe the specific decomposition algorithms in stage 1. Specifically, we introduce the custom algorithm for the sales decomposition of JD.com for the practical case, and apply the classic STL algorithm to the forecast on the public electricity dataset.

Figure 7 Illustration of the Concrete Model in Stage 2



3.3.1. Stage 2: The ML Module for Improvement In stage 2, we utilize the MQ-CNN proposed by Wen et al. (2017) to process empirical data and a weight module with residual connection to generate the weighted combination function for accuracy improvement. Let T denote the length of historical data, then Figure 7 presents the detailed structure when $T = H = 3$.

Basic ML Module of MQ-CNN The lower-left corner of Figure 7 details the MQ-CNN module. The historical features $(\mathbf{x}, \mathbf{y}) = \{(x_{t-k}, y_{t-k}), \forall k \in \{0, \dots, T-1\}\}$ are first put into a WaveNet

module as encoder. The WaveNet algorithm is a CNN-based auto-regression algorithm widely applied in time series forecasting, and we refer the readers to Oord et al. (2016) if interested. Afterwards, the outputs of WaveNet, $\mathbf{h} = \{h_{t-k}, \forall k \in \{0, \dots, T-1\}\}$, are sent into two streams. In the first stream, the algorithm transforms h_t to c_a , which stays stable for different forecasting periods and describes the global information about the historical time series. Meanwhile, the output vector \mathbf{h} is concatenated and then transformed into vector \mathbf{c} of size H , i.e., $\mathbf{c} = \{c_{t+j}, \forall j \in \{1, \dots, H\}\}$. Individual elements within this vector present the historical information for specific forecasting periods and therefore are considered local historical information. For example, c_{t+j} presents the information for horizon $t+j$, and c_{t+j} is likely to differ with c_{t+k} when $k \neq j$. And finally, above variables as well as additional features (such as the date of forecast, denoted by $x_{t+j}, \forall j \in \{1, \dots, H\}$) are put into an MLP module to forecast the residuals $\boldsymbol{\varepsilon} = \{\varepsilon_{t+j}, \forall j \in \{1, \dots, H\}\}$.

Weight Module With the residuals as input, the following module aims to output the weights that apply to the preliminary decompositions. Remind that we incorporate the summing-up constraint to reduce the dimension of the feasible region for weight parameters. The weight module achieves this through two layers. First, we transform the input residuals through a Softmax layer and get the original weight $w_{i,t+j}^{(0)}$ for component i and horizon $t+j$. Mathematically,

$$w_{i,t+j}^{(0)} = \text{Softmax}(\boldsymbol{\varepsilon}_{t+j}) = \frac{\exp(\varepsilon_{i,t+j})}{\sum_k \exp(\varepsilon_{k,t+j})},$$

where $\exp(\cdot)$ denote the exponential function with natural logarithm e . Obviously, $\sum_i \hat{w}_{i,t+j}^{(0)} = 1$. Then we normalize $w_{i,t+j}^{(0)}$ and get the modified weights by

$$w_{i,t+j} = \alpha w_{i,t+j}^{(0)} + 1 - \frac{\alpha}{N}, \quad (4)$$

where N is the number of components from preliminary decomposition, α is a pre-determined parameter controlling the size of the weight interval. Then under Eq. (5), we have $\sum_i w_{i,t+j} = N, \forall j \in \{1, \dots, H\}$, hence the summing-up constraint is satisfied. Moreover, Eq. (5) also restrict the feasible region of $w_{i,t+j}$ to $[1 - \frac{\alpha}{N}, 1 + \alpha - \frac{\alpha}{N}]$, of which the size increases with α . Finally, the modified weights and the residuals, together with the preliminary predictions, combine to output the final overall prediction, i.e.,

$$\hat{y}_{t+j} = w_{i,t+j} \hat{l}_{i,t+j} + \varepsilon_{t+j}, \quad \forall i \in \{1, \dots, N\}, j \in \{1, \dots, H\}.$$

3.3.2. Stage 1: Custom Sales Decomposition in the Practical Case As noted before, we implement the W-R algorithm in two cases. The practical case is the sales prediction for JD.com, one of China's largest online retailers. Following Divakar et al. (2005), Abolghasemi et al. (2020)

and practical experience, we decompose the sales into baseline, promotion- and festival-related components in the first stage, which follow different logic and are generated individually.

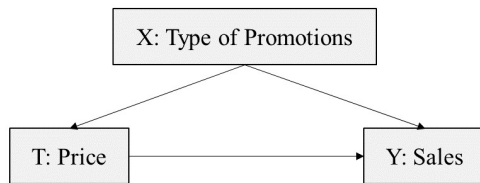
Baseline The baseline indicates regular sales without promotion or specific events. We utilize the FFORMA algorithm proposed by Montero-Manso et al. (2020), which use XGBoost from Chen and Guestrin (2016) to generate a series of weight parameters on alternative forecasting methods. Let $w_m(f_n)$ and $L_m(f_n)$ denote the weight and loss for the n th sample with features f_n and forecasting model m , then the XGBoost model outputs $w_m(f_n)$ to minimize $Loss = \sum_n \sum_m w_m(f_n) \times L_m(f_n)$ in training. When predicting with input feature f_k , the weight parameter $w_m(f_k)$ is the automatically generated by the XGBoost model, and the final prediction for baseline sales, $\hat{l}_b(f_k)$, is a weighted combination of $\hat{l}_m(f_k)$, the original forecasting results of alternative models. Mathematically,

$$\hat{l}_b(f_k) = \sum_m w_m(f_k) \times \hat{l}_m(f_k). \quad (5)$$

As we only focus on regular sales, we omit the spikes induced by promotions or events within the sales data in the training of the numerical experiments. The alternative forecasting models include the moving average (MA), weighted MA, ETS, and ARIMA methods, all of which are classical statistical algorithms with wide application in practice (Chuang et al. 2021). More details on the alternative statistical methods and FFORMA algorithm are given in EC.2.1 and EC.2.2, and we refer the readers to Hyndman and Athanasopoulos (2021) and Montero-Manso et al. (2020) for more details if interested.

Promotion Promotion is an intricate marketing activity with the highest expenditure in the retail industry (van Heerde and Neslin 2008). To capture the complex impacts of price discount and promotion type on sales (as shown in Figure 8), we use Double Machine Learning (DML for short) to eliminate the impacts of promotion type as well as other confounding variables in predicting the promotion-induced sales. Similarly, we briefly introduce the model here and refer the readers to Chernozhukov et al. (2018) for more detail.

Figure 8 Casual Relationship among Price, Promotion Type and Sales



The theoretical foundation of DML is simple mathematics in causal inference. Suppose X is the control variable (i.e., promotion type), Y is the outcome variable, T is the treatment variable, W

denotes other confounding variables (e.g., date, original price, and weekdays in our experiment). Then following the partially linear regression model in Robinson (1988), we have

$$\begin{aligned} Y &= \theta(X, W)T + f_0(X, W) + \varepsilon_0, \\ T &= f_1(X, W) + \varepsilon_1, \end{aligned}$$

where $\varepsilon_0, \varepsilon_1$ are unobserved noises such that $E[\varepsilon_0|X, W, T] = 0$, and $E[\varepsilon_1|X, W, \varepsilon_0] = 0$. The goal is to estimate the conditional average treatment effect of sample x , i.e., $\hat{\theta}(x) = E[\theta(X, W)|X = x]$. After some simple math calculations, Oprescu et al. (2018) found that

$$E[\tilde{Y}|X, \tilde{T}] = \theta(X) \cdot \tilde{T},$$

where $\tilde{Y} = Y - f_0(X, W)$ and $\tilde{T} = T - f_1(X, W)$. Therefore we can get $\hat{\theta}(X)$ by regressing \tilde{Y} on \tilde{T} locally around $X = x$. Then the detailed procedures for DML calculation are as follows.

1. Use ML algorithm to estimate Y and T based on X and W , and get $\hat{f}_0(X, W)$ and $\hat{f}_1(X, W)$;
2. Calculate the residuals \tilde{Y} and \tilde{T} ;
3. Use another ML algorithm to regress \tilde{Y} on \tilde{T} and get the estimation $\hat{\theta}(X)$.

Following the LinearDML in Battocchi et al. (2019), we use gradient-boosting decision tree (GBDT) from Friedman (2001) in Stage 1 and linear regression in Stage 3 in practice. Moreover, we apply $Y = \log(\text{sales})$ and $T = \log(\text{price})$ in the experiment, which makes $\hat{\theta}(X)$ exactly the price elasticity over sales (Kaplan et al. 2011).

Festival The final module captures the impacts of shopping festivals. These festivals are pre-determined in levels by the marketing department of JD.com, e.g., *S level* for the *618 and 1111 Shopping Festivals*, *A level* for the *Valentine's Day and School Season*. The festival-related sales l_f are forecasted by a simple linear regression model, and the prediction $\hat{l}_f = \beta \hat{l}_b$, where β is the festival factor, and \hat{l}_b is the prediction of baseline sales. According to the historical data during previous festivals of the same level, $\beta = \frac{l_{actual} - \hat{l}_b}{\hat{l}_b}$, where l_{actual} is the actual sales, and \hat{l}_b is the corresponding prediction on baseline.

3.3.3. Stage 1: STL Algorithm for the Public Case To validate the effectiveness and scalability of the W-R algorithm, we apply the classical STL algorithm (Seasonal-Trend decomposition procedure based on Loess, proposed by Cleveland et al. 1990) on a public electricity dataset. In accordance with previous sections, we briefly introduce the Loess method, a basic method within STL algorithm, and the general procedure of the STL algorithm here, and we refer the readers to EC.2.4 and Cleveland et al. (1990) for more details.

The Loess Method Loess algorithm is a weighted variant of the K-Nearest Neighbor (KNN) method with additional parameters q , d , and δ . Mathematically, suppose it aims to predict $y(x)$ with samples $\{(x_i, y_i), \forall i \in \{1, \dots, T\}\}$. Then following the KNN algorithm, we choose the q samples closest to x , denoted by S . For each $x_i \in S$, we calculate the weights \mathbf{v} through a given function $W(\cdot)$ and serves as a normalization parameter. Mathematically,

$$v_i(x) = \delta W\left(\frac{|x_i - x|}{\lambda_q(x)}\right), \text{ where } \lambda_q(x) = \begin{cases} \max(|x_i - x|), \forall x_i \in S & \text{if } q \leq T \\ \max(|x_i - x|)^{\frac{q}{n}}, \forall x_i \in S & \text{if } q > T \end{cases},$$

where $W(\cdot)$ is often modeled as the tricube weight function (i.e., $W(x) = (1 - x^3)^3$). And finally, we fit \mathbf{v} by a polynomial function of degree d , and get the result of Loess algorithm.

Calculation Procedure of STL In STL algorithm, $\mathbf{l} = \mathbf{l}_T + \mathbf{l}_S + \mathbf{l}_R$, where \mathbf{l} is the time series, \mathbf{l}_T , \mathbf{l}_S and \mathbf{l}_R denote the trend, seasonality and residual components, respectively. Specifically, the STL algorithm mainly includes two iterative loops, an outer loop to calculate \mathbf{l}_R , and an inner loop to estimate \mathbf{l}_T and \mathbf{l}_S . The general calculation procedure is as follows.

1. Initialization: set $\mathbf{l}_T = 0$.
2. Inner Loop:
 - (a) Use Loess to regress $\mathbf{l} - \mathbf{l}_T$, and get \mathbf{C} ;
 - (b) Use MA and Loess to filter \mathbf{C} and get \mathbf{L} , and update $\mathbf{l}_S = \mathbf{C} - \mathbf{L}$;
 - (c) Use Loess to regress $\mathbf{l} - \mathbf{l}_S$ and get \mathbf{l}_T .
3. Outer Loop: Calculate $\mathbf{l}_R = \mathbf{l} - \mathbf{l}_T - \mathbf{l}_S$.
4. Repeat the inner and outer loops until the termination condition.

4. Numerical Experiment and Results

This section presents the numerical results. Section 4.1 introduce the data and experiment settings, and Section 4.2 reports the numerical results. Finally, in Section 4.3, we analyze the underlying mechanism from the algorithm's outputs, providing evidence for the algorithm's effectiveness.

4.1. Experiment Design

4.1.1. Loss Function and Evaluation Indicators As mentioned in Section 3.1, the W-R algorithm predicts quantiles in multiple forecasting horizons. Accordingly, following Wen et al. (2017), we adopt the quantile loss function

$$Loss(y, \hat{y}) = p(y - \hat{y})_+ + (1 - p)(\hat{y} - y)_+,$$

where $(\cdot)_+ = \max(0, \cdot)$, y is the actual value, \hat{y} is the forecasted value of quantile p . In the experiments, we select $p = 0.5$, the most widely applied parameter, and the minimizer of loss is the

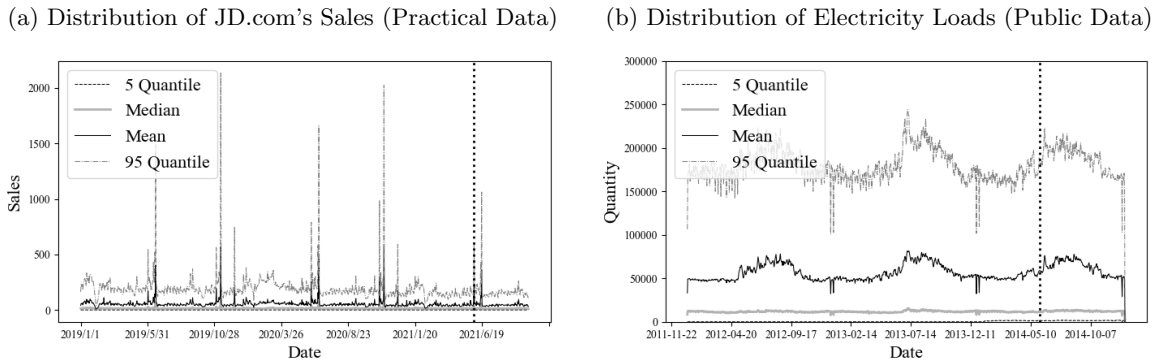
median of the predictive distribution (Fattah et al. 2018). Remember that t denotes the forecasting time, H is the length of the forecasting horizon, then we evaluate the models' performance through the two indicators, Root Median Square Error (RMSE for short) and P50_QL. Mathematically,

$$RMSE = \sqrt{\text{average} \left(\sum_{i,t} (y_{i,t} - \hat{y}_{i,t})^2 \right)}, \quad P50_QL = \frac{\sum_{i,t} \left| \sum_{j=1}^H \hat{y}_{i,t+j} - \sum_{j=1}^H y_{i,t+j} \right|}{2 \sum_{i,t} \left| \sum_{j=1}^H \hat{y}_{i,t+j} \right|},$$

where $y_{i,t+j}$ and $\hat{y}_{i,t+j}$ denote the actual and forecasted value for sample i in period $t+j$, respectively. These indicators are essentially similar to the *Root Mean Square Error* and *Weighted Mean Absolute Percentage Error*, just replacing the mean with the median. Specifically, RMSE is a general indicator evaluating the detailed performance on separate periods, and P50_QL is an aggregated indicator widely applied in multi-horizon forecasting (e.g., in Wen et al. 2017, Salinas et al. 2020).

4.1.2. Data and Descriptive Statistics In the practical case, we utilize the data of 16,973 individual products from 298 categories in a given distribution center of JD.com, and the specific product information is anonymous for security reasons. Figure 9a presents the distribution of individual sales over time, where the dotted vertical line divides the training and test sets. As the products are launched for sale at different times, we randomly select 72 samples for each product to avoid the influence of bias from data in training. Generally speaking, the sales are significantly right-skewed, and the products with higher sales are more volatile. Specifically, the indicator of 95 quantiles has two significant peaks every year, corresponding to the *618* and *11-11 Shopping Festivals* that occur in June and November. Therefore, the custom decomposition algorithm of JD.com is more effective than other general algorithms, as it considers the significant influencing factors of sales, i.e., the promotion and festival.

Figure 9 Distribution of the Time Series in Numerical Experiments



The public dataset, meanwhile, is the electricity loads data provided by UCI (2015). The dataset consists of the time series data of 370 electrical clients from early 2011 to late 2014 and has

been widely applied in relevant literature (e.g., Ömer Faruk Ertugrul 2016, Shih et al. 2019, Chen et al. 2020, Salinas et al. 2020). We calculate the daily time series as the forecast target in our experiment. As shown in Figure 9b, the electricity loads are also right-skewed and highly volatile, similar to the sales in Figure 9a. However, there are no significant peaks induced by specific events. Hence we utilize the STL method as the preliminary decomposition algorithm. As both the STL and W-R algorithms consider the residual component, here we only use the trend and seasonality components from STL as the initial predictions on components.

4.1.3. Features and Parameters As listed in Table EC.3, Section EC.3.1, the features for the practical case include historical data on sales, prices, and promotions, and extra information on time and products. Specifically, in the practical case, we consider four actual promotion types in JD.com: direct discount, seckill (a time/quantity-limited discount), X off on purchases over Y for a variety of products, and bundled discount, in addition to the classical historical and additional features. As for the experiment on public datasets, we only utilize the original time series, client information, and time features as other data are unavailable.

The parameters, as listed in Table EC.4, EC.3.1, are all common parameters in similar researches. Briefly speaking, for the practical case, we use the historical information of the past 72 days to forecast the sales of the following 24 days from 1st, June to September 2021. On the public dataset, we predict the time series in a month starting from three pre-determined forecasting dates, 1st June, 1st July, and 1st August 2014, with the historical data before the date as the training set. To ensure the robustness of all results, we replicate each experiment 10 times and report the average of evaluation indicators. In each experiment, we train the model from 10 to 50 times and report the evaluation indicators with the best performance. We utilize tensorflow-based python programming in both experiments, and the open-source packages used are listed in Section EC.3.2.

4.2. Numerical Results

4.2.1. The Impact of α Before evaluating the accuracy, we need to determine α in Eq. (5), the parameter controlling the scope of weights. Inspired by the theoretical results, we restrict $\alpha \in [0, N]$, and the results on practical and public data are given by Tables 2 and 3, respectively.

Note that the weights are equal to 1 when $\alpha = 0$, and the model is just a simple addition with an additive residual. The feasible region of weights increases with α , and the W-R algorithm achieves the best performance in both cases when $\alpha = 1$. This phenomenon validates the Conjecture 1 in Section 3.2. First, α should be positive to ensure the effectiveness of the weight mechanism. In addition, when α makes the weights in a proper, moderate interval around 1, the estimates on

Table 2 Model Performance with Different α
(Practical Data, $N = 3$)

Value of α	RMSE	P50_QL	Scope of Weight
0	2.1659	0.2089	1
0.5	2.1544	0.2067	[0.83, 1.33]
1	2.0396	0.2001	[0.67, 1.67]
2	2.1595	0.2062	[0.33, 2.33]
3	2.1583	0.2092	[0, 3]

Table 3 Model Performance with Different α
(Public Data, $N = 2$)

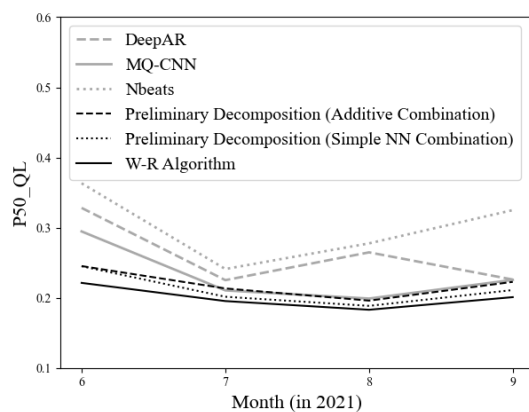
Value of α	RMSE	P50_QL	Scope of Weight
0	0.7106	0.0464	1
0.5	0.6821	0.0303	[0.75, 1.25]
1	0.4682	0.0261	[0.50, 1.50]
1.5	1.5263	0.0651	[0.25, 1.75]
2	1.4264	0.0853	[0, 2]

components are less biased, making the total prediction more accurate. Moreover, by comparing the results from practical and public cases, the improvements led by the W-R algorithm and the weight mechanism are both more significant when the simple additive function shows poor performance.

4.2.2. Model Performance Table 4 and Figure 10 present the performance comparison among models in the practical case. In addition to the W-R algorithm with $\alpha = 1$, we also consider three streams of benchmarks here. The first stream serves as a general benchmark and includes two popular existing algorithms, DeepAR and N-BEATS. The second stream aims to validate the idea of combining ML and preliminary decompositions and consists of the W-R algorithm’s basic modules, including the MQ-CNN and the simple addition of the custom sales decomposition algorithm, named *Preliminary Decomposition I*. The final benchmark is *Preliminary Decomposition II*, a variation of the W-R algorithm which uses a simple MLP to separately output the weights and residual, to validate the effect of residual connection.

Table 4 Comparison on Model Performance
(Practical Data)

Algorithm	RMSE	P50_QL
MQ-CNN	2.5107	0.2324
Preliminary Decomposition I (Additive Combination)	2.4104	0.2193
Preliminary Decomposition II (Simple MLP Combination)	2.3303	0.2115
W-R Algorithm ($\alpha = 1$)	2.0396	0.2001
DeepAR	2.6334	0.2610
N-BEATS	2.7522	0.3017

Figure 10 Model Performance Over Time
(Practical Data)

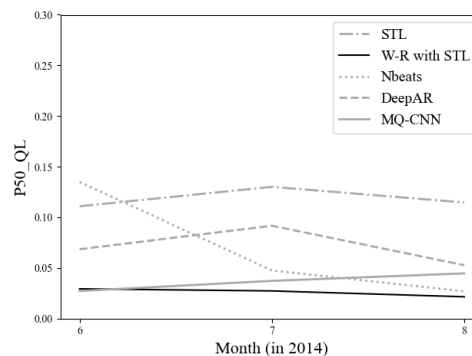
The results are satisfying in every sense. First, we validate the importance of custom decomposition for sales. Even the simplest version, *Preliminary Decomposition I* with simple additive

combination, achieves better performance than pure ML algorithms, especially during big promotions (i.e., the *618 Shopping Festival* in June). On the basis of such a good prediction, the W-R algorithm steadily improves the forecasting accuracy, ranging from 2.60% to 84.79% in absolute P50_QL, and 0.08 to 0.62 in absolute RMSE by month (see Table EC.6 for specific statistics). Overall, the relative accuracy improvement is 8.76% in P50_QL, and 15.38% in RMSE. While the approach using simple MLP to output the weights and residuals also improves the preliminary decomposition, the extent of improvement is less significant than our algorithm. Therefore, the specific structure of residual connection in the W-R algorithm is necessary, in addition to the idea of modification through weight and residual.

Table 5 Comparison on Model Performance (Public Data)

Algorithm	RMSE	P50_QL
STL with Additive Combination	2.2967	0.1186
W-R Algorithm ($\alpha = 1$)	0.4682	0.0261
MQ-CNN	0.6265	0.0364
DeepAR	1.2097	0.0710
N-BEATS	1.1203	0.0698

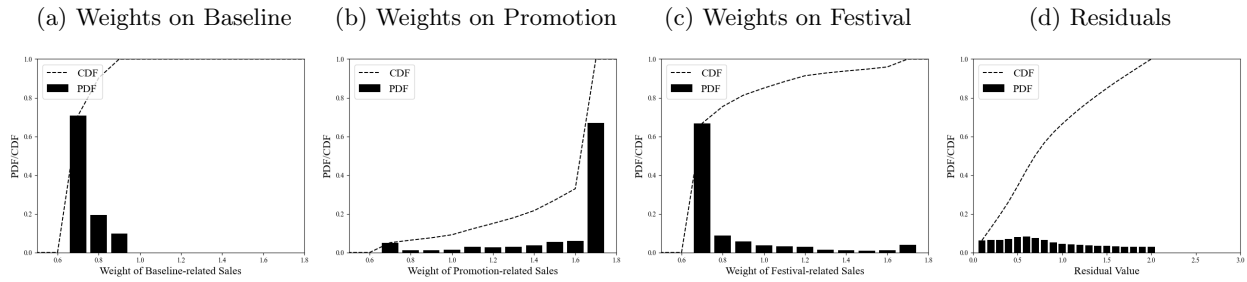
Figure 11 Model Performance Over Time (Public Data)



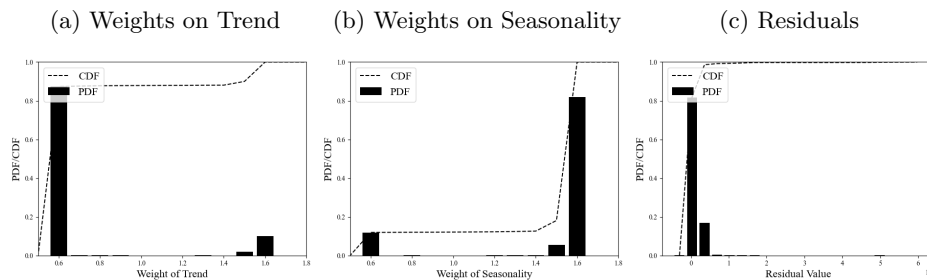
We further check the robustness of the W-R algorithm’s superiority through experiments on the public dataset. As shown in Table 5 and Figure 11, the numerical results on public datasets validate the poor performance of STL, which is not surprising, and the significant improvement induced by the W-R algorithm, which is of 9.25%(77.99%) in absolute(relative) P50_QL and 1.8285(79.62%) in absolute(relative) RMSE. The improvement in accuracy certainly comes from the ML structure, i.e., the MQ-CNN algorithm, which performs the second best among the alternatives.

4.3. Post-hoc Analysis on Undelying Mechanism

We finally check the underlying mechanism of the W-R algorithm in the numerical experiments through post-hoc analysis. We start with the practical sales forecast case and draw the weight parameters’ probability distribution in Figure 12. Note that the weights of baseline sales are all less than 1; that is, the W-R algorithm thinks the custom decomposition algorithm overestimates the baseline sales. The idea is essentially appropriate. Remind that we predict the baseline through a combination of naive statistical methods. While we have deleted the spikes closely related to exogenous variables, it is likely that we missed some small promotions, making the original baseline include some sales from small promotions.

Figure 12 Distribution of the Weights and Residuals (Practical Data)

The weights on the promotions and festivals are almost opposite in distribution. In general, the W-R algorithm amplifies the effects of promotions on sales but reduces those of festivals. This phenomenon makes sense as the simple linear regression model for the festival does not exclude the impacts of simultaneous promotions. As we all know, it isn't easy to distinguish between highly relevant promotions and festivals; however, the W-R algorithm has a different view of these two components compared to human predictions. Finally, following a nearly uniform distribution from 0 to 2, the residuals are relatively stable compared to the weights and relatively small in contrast to other components. Therefore, we infer that the improvement of forecasting accuracy mainly comes from the redistribution of components through the weight parameter in the practical case.

Figure 13 Distribution of the Weights and Residuals (Public Data)

For the experiment on the public dataset, we depict the distribution of output parameters in Figure 13. First, as illustrated in Figures 13a and 13b, the W-R algorithm modifies the weights of trend and seasonality components. In most cases, the trend component is reduced while the seasonality component is magnified. However, the trend and seasonality components do not explain the whole time series. As shown in Figure 13c, the residuals are large in values, with an average of 39,290.41. Apparently, we should search for additional explanatory components to improve the existing algorithm, e.g., the unit price for electricity.

5. Conclusion and Discussion

This research is inspired by the persisting conflict between accuracy and interpretability in time series forecasts. In response, we first quantitatively define interpretability in data-driven forecasting. The innovative definition includes the interpretability of inputs and the function, making distinct algorithms comparable in interpretability. We then build a unifying framework and systematically review the existing algorithms. We find that while there are several hybrid interpretable ML algorithms, these algorithms usually rely on strong statistical assumptions or theoretical structures, which restricts the potential of ML. In particular, the additive combination function in most decomposition-based algorithms implies an assumption of independence, and the algorithms' performance would be compromised when the components are correlated.

Accordingly, we propose a novel W-R algorithm for time series forecasting, which has specific advantages in multi-dimensional accuracy and interpretability. First, integrating the decomposition-based and ML approaches allows the algorithm to be accurate in extensive cases, even when the preliminary decompositions are inappropriate. Moreover, the theoretical analysis of the weighted mechanism reveals the possibility of reducing the prediction errors of components, implying that the modified estimates on the components from the W-R algorithm are likely to improve with proper restrictions. Finally, in contrast with other hybrid algorithms, the W-R algorithm utilizes ML to generate the parameters in a weighted combination function rather than the direct predictions. According to the innovative definition of interpretability, the weighted combination function is just as interpretable as the simple addition, and hence our algorithm is just as interpretable as other algorithms with additive combination functions.

Compared with existing literature, the W-R algorithm provides an innovative perspective for combining the classic statistical and black-box ML algorithms. Based on a weighted combination function, the algorithm improves the accuracy of decomposition-based algorithms and the interpretability of ML algorithms. Moreover, the W-R algorithm possesses great generalization ability in the application, and the resulting accurate predictions on components have significant managerial implications for firms. At this point, the W-R algorithm has been incorporated by JD's intelligent forecasting system, and the resulting predictions on promotion and festivals serve as important guides for marketing activities.

References

Abolghasemi M, Beh E, Tarr G, Gerlach R (2020) Demand forecasting in supply chain: The impact of demand volatility in the presence of promotion. *Computers & Industrial Engineering* 142:106–380, ISSN 0360-8352.

- Ahmed NK, Atiya AF, Gayar NE, El-Shishiny H (2010) An empirical comparison of machine learning models for time series forecasting. *Econometric Reviews* 29(5-6):594–621.
- Assimakopoulos V, Nikolopoulos K (2000) The theta model: A decomposition approach to forecasting. *International Journal of Forecasting* 16:521–530.
- Battocchi K, Dillon E, Hei M, Lewis G, Oka P, Oprescu M, Syrgkanis V (2019) EconML: A Python Package for ML-Based Heterogeneous Treatment Effects Estimation. <https://github.com/microsoft/EconML>, version 0.x.
- Bertsimas D, Delarue A, Jaillet P, Martin S (2019) Optimal explanations of linear models. *CoRR* URL <http://dx.doi.org/https://doi.org/10.48550/arXiv.1907.04669>.
- Bertsimas D, Dunn J, Wang Y (2021) Near-optimal nonlinear regression trees. *Operations Research Letters* 49:201–206.
- Borovykh A, Bohte S, Oosterlee C (2019) Dilated convolutional neural networks for time series forecasting. *Journal of Computational Finance* 22(4):73–101.
- Box GEP, Jenkins GM (1970) *Time Series Analysis: Forecasting and Control* (Holden-Day, San Francisco).
- Breiman L (2001) Random forests. *Machine Learning* 45:5–32.
- Breiman L, Friedman JH, Olshen R, Stone CJ (1984) *Classification and Regression Trees* (Belmont, California: Wadsworth).
- Chen T, Guestrin C (2016) Xgboost: A scalable tree boosting system. *Proceedings of the 22nd ACM SIGKDD International Conference on Knowledge Discovery and Data Mining*, 785–794, KDD '16 (New York, NY, USA: Association for Computing Machinery).
- Chen Y, Kang Y, Chen Y, Wang Z (2020) Probabilistic forecasting with temporal convolutional neural network. *Neurocomputing* 399:491–501.
- Chernozhukov V, Chetverikov D, Demirer M, Duflo E, Hansen C, Newey W, Robins J (2018) Double/debiased machine learning for treatment and structural parameters. *The Econometrics Journal* 21(1):C1–C68.
- Cho K, van Merriënboer B, Gulcehre C, Bahdanau D, Bougares F, Schwenk H, Bengio Y (2014) Learning phrase representations using RNN encoder–decoder for statistical machine translation. *Proceedings of the 2014 Conference on Empirical Methods in Natural Language Processing (EMNLP)*, 1724–1734.
- Chuang HHC, Chou YC, Oliva R (2021) Cross-item learning for volatile demand forecasting: An intervention with predictive analytics. *Journal of Operations Management* 67(7):828–852.
- Cleveland R, Cleveland W, McRae J, Terpenning I (1990) Stl: a seasonal-trend decomposition procedure based on loess. *Journal of Official Statistics* 6:3–73.
- De Gooijer JG, Hyndman RJ (2006) 25 years of time series forecasting. *International Journal of Forecasting* 22(3):443–473.
- Divakar S, Ratchford BT, Shankar V (2005) Chan4cast: A multichannel, multiregion sales forecasting model and decision support system for consumer packaged goods. *Marketing Science* 24(3):334–350.
- Dokumentov A, Hyndman RJ (2022) Str: Seasonal-trend decomposition using regression. *INFORMS Journal on Data Science* 1(1):50–62.

- Du M, Liu N, Hu X (2020) Techniques for interpretable machine learning. *Communications of the ACM* 63(1):68–77.
- Dudek G (2022) Std: A seasonal-trend-dispersion decomposition of time series. *CORR* URL <http://dx.doi.org/https://doi.org/10.48550/arXiv.2204.10398>.
- Fattah J, Ezzine L, Aman Z, Moussami H, Lachhab A (2018) Forecasting of demand using arima model. *International Journal of Engineering Business Management* 10, URL <http://dx.doi.org/10.1177/1847979018808673>.
- Friedman JH (2001) Greedy function approximation: A gradient boosting machine. *Annals of Statistics* 29:1189–1232.
- Guo X, Grushka-Cockayne Y, De Reyck B (2022) Forecasting airport transfer passenger flow using real-time data and machine learning. *Manufacturing & Service Operations Management* Ahead of Print.
- He K, Zhang X, Ren S, Sun J (2016) Deep residual learning for image recognition. *2016 IEEE Conference on Computer Vision and Pattern Recognition (CVPR)*, 770–778, URL <http://dx.doi.org/10.1109/CVPR.2016.90>.
- Hewamalage H, Bergmeir C, Bandara K (2021) Recurrent neural networks for time series forecasting: Current status and future directions. *International Journal of Forecasting* 37(1):388–427.
- Hochreiter S, Schmidhuber J (1997) Long short-term memory. *Neural Computation* 9(8):1735–1780.
- Holt CC (1957) Forecasting seasonals and trends by exponentially weighted averages Reprinted with discussion in 2004. *International Journal of Forecasting*, 20, 5-13.
- Hyndman R, Athanasopoulos G (2021) *Forecasting: principles and practice* (Melbourne, Australia: OTexts), URL <https://otexts.com/fpp3/>.
- Kaplan U, Türkay M, Karasözen B, Biegler LT (2011) Optimization of supply chain systems with price elasticity of demand. *INFORMS Journal on Computing* 23(4):557–568.
- Ke G, Meng Q, Finely T, Wang T, Chen W, Ma W, Ye Q, Liu TY (2017) Lightgbm: A highly efficient gradient boosting decision tree. *Advances in Neural Information Processing Systems 30 (NIP 2017)*.
- Kim KJ (2003) Financial time series forecasting using support vector machines. *Neurocomputing* 55(1):307–319.
- Lea C, Vidal R, Reiter A, Hager GD (2016) Temporal convolutional networks: A unified approach to action segmentation. *Computer Vision – ECCV 2016 Workshops*, 47–54 (Cham: Springer International Publishing).
- Lim B, Arık SÖ, Loeff N, Pfister T (2021) Temporal fusion transformers for interpretable multi-horizon time series forecasting. *International Journal of Forecasting* 37(4):1748–1764.
- Lin Y, Koprinska I, Rana M (2021) Ssdnet: State space decomposition neural network for time series forecasting. *2021 IEEE International Conference on Data Mining (ICDM)*, 370–378.
- Miller T (2019) Explanation in artificial intelligence: Insights from the social sciences. *Artificial Intelligence* 267:1–38.
- Molnar C (2022) *Interpretable Machine Learning*. 2 edition, URL christophm.github.io/interpretable-ml-book/.

- Montero-Manso P, Athanasopoulos G, Hyndman RJ, Talagala TS (2020) Fforma: Feature-based forecast model averaging. *International Journal of Forecasting* 36(1):86–92.
- Murdoch WJ, Singh C, Kumbier K, Abbasi-Asl R, Yu B (2019) Definitions, methods, and applications in interpretable machine learning. *Proceedings of the National Academy of Sciences* 116(44):22071–22080.
- Olivares KG, Challu C, Marcjasz G, Weron R, Dubrawski A (2022) Neural basis expansion analysis with exogenous variables: Forecasting electricity prices with nbeatsx. *International Journal of Forecasting* .
- Oord A, Dieleman S, Zen H, Simonyan K, Vinyals O, Graves A, Kalchbrenner N, Senior A, Kavukcuoglu K (2016) Wavenet: A generative model for raw audio. *CORR* URL <http://dx.doi.org/https://doi.org/10.48550/arXiv.1609.03499>.
- Opreescu M, Syrgkanis V, Wu ZS (2018) Orthogonal random forest for heterogeneous treatment effect estimation. *CoRR* abs/1806.03467, URL <http://arxiv.org/abs/1806.03467>.
- Oreshkin BN, Carpov D, Chapados N, Bengio Y (2019) N-BEATS: neural basis expansion analysis for interpretable time series forecasting. *arXiv* abs/1905.10437.
- Robinson PM (1988) Root-n-consistent semiparametric regression. *Econometrica* 56:931–954.
- Salinas D, Flunkert V, Gasthaus J, Januschowski T (2020) Deepar: Probabilistic forecasting with autoregressive recurrent networks. *International Journal of Forecasting* 36(3):1181–1191.
- Sastri T (1985) A state space modeling approach for time series forecasting. *Management Science* 31(11):1451–1470.
- Shih SY, Sun FK, yi Lee H (2019) Temporal pattern attention for multivariate time series forecasting. *Machine Learning* 108:1421–1441.
- Snyder RD, Ord JK, Koehler AB, McLaren KR, Beaumont AN (2017) Forecasting compositional time series: A state space approach. *International Journal of Forecasting* 33(2):502–512, ISSN 0169-2070.
- Taylor SJ, Letham B (2018) Forecasting at scale. *The American Statistician* 72(1):37–45.
- Triebe O, Hewamalage H, Pilyugina P, Laptev N, Bergmeir C, Rajagopal R (2021) Neuralprophet: Explainable forecasting at scale. *CORR* URL <http://dx.doi.org/https://doi.org/10.48550/arXiv.2111.15397>.
- UCI (2015) Uci machine learning repository: Electricityloaddiagrams20112014 data set. Website, <http://archive.ics.uci.edu/ml/datasets/ElectricityLoadDiagrams20112014>.
- van Heerde HJ, Neslin SA (2008) *Sales Promotion Models*, 107–162 (Boston, MA: Springer US).
- Vaswani A, Shazeer N, Parmar N, Uszkoreit J, Jones L, Gomez AN, Kaiser Lu, Polosukhin I (2017) Attention is all you need. *Advances in Neural Information Processing Systems*, volume 30 (Curran Associates, Inc.).
- Wen R, Torkkola K, Narayanaswamy B, Madeka D (2017) A multi-horizon quantile recurrent forecaster. *31st Conference on Neural Information Processing Systems (NIPS 2017), Time Series Workshop* (Red Hook, NY, USA: Curran Associates Inc.).
- Winters PR (1960) Forecasting sales by exponentially weighted moving averages. *Management Science* 6:324–342.
- Wittink D, Addona M, Hawkes W, , Porter J (1988) Scan*pro: The estimation, validation and use of promotional effects based on scanner data. Internal Paper.

Zhou Q, Liao F, Mou C, Wang P (2018) Measuring interpretability for different types of machine learning models. *Trends and Applications in Knowledge Discovery and Data Mining*, 295–308 (Cham: Springer International Publishing), ISBN 978-3-030-04503-6.

Ömer Faruk Ertugrul (2016) Forecasting electricity load by a novel recurrent extreme learning machines approach. *International Journal of Electrical Power & Energy Systems* 78:429–435.

E-Companions

EC.1. Mathematical Proofs for Section 3.2

EC.1.1. Proof of Proposition 1

When $N = 2$, the weighted combination function is $\hat{y} = w\hat{l}_1 + (2-w)\hat{l}_2$, and the additive combination function is a special case with $w = 1$. Then the optimization problem is

$$\min_w E[y - \hat{y}] \Leftrightarrow \min_w L = (y - \hat{y})^2 = \left(y - w\hat{l}_1 - (2-w)\hat{l}_2\right)^2.$$

We then calculate the first and second order of derivatives, i.e.,

$$\begin{aligned}\frac{\partial L}{\partial w} &= 2 \left(y - w\hat{l}_1 - (2-w)\hat{l}_2\right) \left(-\hat{l}_1 + \hat{l}_2\right), \\ \frac{\partial^2 L}{\partial w^2} &= 2 \left(-\hat{l}_1 + \hat{l}_2\right)^2 \geq 0.\end{aligned}$$

Then when $\hat{l}_1 = \hat{l}_2$, $\frac{\partial L}{\partial w} = \frac{\partial^2 L}{\partial w^2} = 0$, the objective function stays constant for all $w \in [0, 2]$. Otherwise, when $\hat{l}_1 \neq \hat{l}_2$, $\frac{\partial^2 L}{\partial w^2} > 0$, the objective function is strictly convex over w . Let $\frac{\partial L}{\partial w} = 0$, we have

$$w^* = \frac{y - 2\hat{l}_2}{\hat{l}_1 - \hat{l}_2}. \quad (\text{EC.1})$$

When the simple addition achieves the best performance, $w^* = 1$, $y = \hat{l}_1 + \hat{l}_2$. Otherwise, $w^* \neq 1$, the weighted combination function performs better than the simple addition. \square

EC.1.2. Proof of Proposition 2

When $N > 2$, the weighted combination function is $\hat{y} = w_1\hat{l}_1 + \hat{l}_2 + \dots + w_{N-1}\hat{l}_{N-1} + (N - w_1 - w_2 - \dots - w_{N-1})\hat{l}_N$, and the additive combination function is a special case with $\mathbf{w} = \mathbf{1}$. Then the optimization problem is

$$\begin{aligned}\min_{\mathbf{w}} |\mathbf{y} - \hat{\mathbf{y}}| &\Leftrightarrow \min_{\mathbf{w}} L = (y - \hat{y})^2 \\ &= \left(y - w_1\hat{l}_1 - w_2\hat{l}_2 - \dots - w_{N-1}\hat{l}_{N-1} - (N - w_1 - w_2 - \dots - w_{N-1})\hat{l}_N\right)^2.\end{aligned}$$

Then obviously, the objective function has a minimum of 0 when $y = w_1^*\hat{l}_1 + w_2^*\hat{l}_2 + \dots + w_{N-1}^*\hat{l}_{N-1} + (N - w_1^* - w_2^* - \dots - w_{N-1}^*)\hat{l}_N$. The optimal weights $\mathbf{w}^* \in \mathbb{R}^{N-2}$ if there's not any other additional constraint. \square

Example: The specific case of numerical experiment In the numerical experiment of our research, we further restrict $w_i^* \in [1 - \frac{\alpha}{N}, 1 - \frac{\alpha}{N} + \alpha] \forall i$, where $\alpha \in [0, N]$. Then in the practical case of sales prediction, $N = 3$, the feasible region of weights is $\{w_1^*, w_2^*, w_3^*\} \in \mathbb{R}$, which satisfying

$$w_1^* \in [1 - \frac{\alpha}{N}, 1 - \frac{\alpha}{N} + \alpha], \quad w_2^* = \frac{y + w_1^*(\hat{l}_3 - \hat{l}_1) - 3\hat{l}_3}{\hat{l}_2 - \hat{l}_3}, \quad w_3^* = N - w_1^* - w_2^*.$$

EC.1.3. Proof of Proposition 3

LEMMA EC.1. *If $\hat{l}_i(w_i - 1)((w_i + 1)\hat{l}_i - 2l_i) < 0$, $|w_i\hat{l}_i - l_i| < |\hat{l}_i - l_i|$, the modified estimation $w_i\hat{l}_i$ is less biased than the original prediction \hat{l}_i .*

Proof:

$$\begin{aligned} |w_i\hat{l}_i - l_i| < |\hat{l}_i - l_i| &\Leftrightarrow (w_i\hat{l}_i - l_i)^2 - (\hat{l}_i - l_i)^2 < 0 \\ &\Leftrightarrow (w_i\hat{l}_i - \hat{l}_i)(w_i\hat{l}_i + \hat{l}_i - 2l_i) < 0 \\ &\Leftrightarrow \hat{l}_i(w_i - 1)((w_i + 1)\hat{l}_i - 2l_i) < 0. \quad \square \end{aligned}$$

When $N = 2$, the weight parameter for component 1 $w_1^* = w^* = \frac{y - 2\hat{l}_2}{\hat{l}_1 - \hat{l}_2}$. According to Lemma EC.1, when $\hat{l}_i > 0$, $w_1^*\hat{l}_1$ is less biased than \hat{l}_1 if and only if

$$\begin{aligned} (w_1^* - 1)((w_1^* + 1)\hat{l}_1 - 2l_1) < 0 &\Leftrightarrow \frac{\hat{l}_1}{(\hat{l}_1 - \hat{l}_2)^2} (y - \hat{l}_1 - \hat{l}_2) (\hat{l}_1^2 + \hat{l}_1(y - 3\hat{l}_2 - 2l_1) + 2l_1\hat{l}_2) < 0 \\ &\Leftrightarrow (y - \hat{l}_1 - \hat{l}_2) g(\hat{l}_1) < 0. \end{aligned}$$

Similarly, the weight parameter for component 2 $w_2^* = 2 - w^* = \frac{2\hat{l}_1 - y}{\hat{l}_1 - \hat{l}_2}$, and

$$\begin{aligned} (w_2^* - 1)((w_2^* + 1)\hat{l}_2 - 2l_2) < 0 &\Leftrightarrow \frac{\hat{l}_2}{(\hat{l}_1 - \hat{l}_2)^2} (y - \hat{l}_1 - \hat{l}_2) (\hat{l}_2^2 + \hat{l}_2(y - 3\hat{l}_1 - 2l_2) + 2l_2\hat{l}_1) < 0 \\ &\Leftrightarrow (y - \hat{l}_1 - \hat{l}_2) g(\hat{l}_2) < 0. \end{aligned}$$

Taking together, we have Proposition 3. Specifically, when $y > \hat{l}_1 + \hat{l}_2$ (or $y < \hat{l}_1 + \hat{l}_2$), component i is less biased after multiplying with the w_i^* if and only if $g(\hat{l}_i) < 0$ (or $g(\hat{l}_i) > 0$). \square

EC.1.4. Proof of Proposition 4

Following Lemma EC.1, when $\hat{l}_i > 0$, $|w_i\hat{l}_i - l_i| < |\hat{l}_i - l_i| \Leftrightarrow (w_i - 1)((w_i + 1)\hat{l}_i - 2l_i) < 0$. Mathematically, let $T(w_i) = (w_i - 1)((w_i + 1)\hat{l}_i - 2l_i) = \hat{l}_i w_i^2 - 2l_i w_i - \hat{l}_i + 2l_i$, which is quadratic over w_i . Moreover, as $(-2l_i)^2 - 4\hat{l}_i(-\hat{l}_i + 2l_i) = 4(\hat{l}_i - l_i)^2 \geq 0$, $T(w_i) = 0$ has two distinct solutions as long as $\hat{l}_i \neq l_i$. We denote these two solutions by $w_i^{[*1]}$ and $w_i^{[*2]}$ with $w_i^{[*1]} < w_i^{[*2]}$.

1. When $l_i > \hat{l}_i$, $w_i^{[*1]} = 1$ and $w_i^{[*2]} = \frac{2l_i}{\hat{l}_i} - 1$. The first scenario in Proposition 4 is proved.
2. Otherwise, when $l_i < \hat{l}_i$, $w_i^{[*1]} = \frac{2l_i}{\hat{l}_i} - 1$ and $w_i^{[*2]} = 1$. The second scenario in Proposition 4 is proved. \square

Here we also briefly discuss the case when $\hat{l}_i < 0$. In this case, $|w_i\hat{l}_i - l_i| < |\hat{l}_i - l_i| \Leftrightarrow (w_i - 1)((w_i + 1)\hat{l}_i - 2l_i) > 0 \Leftrightarrow T(w_i) > 0$, and the two solutions of $T(w_i) = 0$ stay the same. We then have Proposition EC.1 as follows.

PROPOSITION EC.1. When $\hat{l}_i < 0$, $|w_i \hat{l}_i - l_i| < |\hat{l}_i - l_i|$ if and only if:

1. $l_i > \hat{l}_i$, and $w_i < 1$ or $w_i > \frac{2l_i}{\hat{l}_i} - 1$;
2. Otherwise, $l_i < \hat{l}_i$, and $w_i < \frac{2l_i}{\hat{l}_i} - 1$ or $w_i > 1$.

It is worth mentioning that this scenario rarely happens in practice for the following two reasons. First, we can always modify the negative estimates to the positive ones by adding a positive constant. Secondly, some time series are impossible to be negative due to the physical characteristics. For example, our numerical experiments are built on sales and electricity loads, which are naturally non-negative.

EC.1.5. Proof of Corollary 1

LEMMA EC.2. In the specific case with $N = 2$, suppose $\hat{l}_1 > \hat{l}_2$. Then component 1 improves as long as component 2 improves.

Proof: In the specific case without residual, $y = l_1 + l_2$. Following the definition of $g(\hat{l}_i)$, we have

$$\begin{aligned} g(\hat{l}_1) - g(\hat{l}_2) &= (\hat{l}_1 - \hat{l}_2) \left(y + \hat{l}_1 + \hat{l}_2 - 2(l_1 + l_2) \right) \\ &= (\hat{l}_1 - \hat{l}_2) \left(\hat{l}_1 + \hat{l}_2 - y \right). \end{aligned}$$

Then when $y > \hat{l}_1 + \hat{l}_2$, $g(\hat{l}_1) - g(\hat{l}_2) < 0$, $g(\hat{l}_1) < 0$ as long as $g(\hat{l}_2) < 0$. Similarly, when $y < \hat{l}_1 + \hat{l}_2$, $g(\hat{l}_1) - g(\hat{l}_2) > 0$, $g(\hat{l}_1) > 0$ as long as $g(\hat{l}_2) > 0$. Taking Proposition 3 together, Lemma EC.2 is proved. \square

Then according to Proposition 3, the conditions for both components to improve become:

1. $y > \hat{l}_1 + \hat{l}_2$ and $g(\hat{l}_2) < 0$;
2. Or the opposite, $y < \hat{l}_1 + \hat{l}_2$ and $g(\hat{l}_2) > 0$.

We analyze the previous two scenarios respectively.

Scenario 1: The first scenario requires $y > \hat{l}_1 + \hat{l}_2$ and $g(\hat{l}_2) < 0$, where

$$g(\hat{l}_2) < 0 \Leftrightarrow y < 3\hat{l}_1 + 2l_2 - \hat{l}_2 - 2\frac{l_2\hat{l}_1}{\hat{l}_2}.$$

Therefore

$$\hat{l}_1 + \hat{l}_2 < y < 3\hat{l}_1 + 2l_2 - \hat{l}_2 - 2\frac{l_2\hat{l}_1}{\hat{l}_2} \rightarrow \hat{l}_1 + \hat{l}_2 < 3\hat{l}_1 + 2l_2 - \hat{l}_2 - 2\frac{l_2\hat{l}_1}{\hat{l}_2} \rightarrow \hat{l}_2 > l_2,$$

and scenario 1 has no-empty solution only if $\hat{l}_2 > l_2$. And we have the following restrictions on the feasible region of \hat{l}_1 and \hat{l}_2 ,

$$\begin{aligned} y = l_1 + l_2 > \hat{l}_1 + \hat{l}_2, \hat{l}_2 > l_2 &\Leftrightarrow \hat{l}_1 < l_1 + l_2 - \hat{l}_2 < l_1, \\ y = l_1 + l_2 > \hat{l}_1 + \hat{l}_2, \hat{l}_1 > \hat{l}_2 &\Leftrightarrow \hat{l}_2 < \frac{l_1 + l_2}{2}. \end{aligned}$$

Moreover, when $\hat{l}_1 > \frac{l_1 + l_2}{2}$, $\hat{l}_1 > y - \hat{l}_1$, and the feasible region of \hat{l}_2 is $(l_2, y - \hat{l}_1)$. As $g(\hat{l}_2)$ is strictly convex over \hat{l}_2 , and

$$\begin{aligned} g(\hat{l}_2 = l_2) &= l_2(l_1 - \hat{l}_1) > 0, \\ g(\hat{l}_2 = y - \hat{l}_1) &= 2(l_1 - \hat{l}_1)(l_1 + l_2 - 2\hat{l}_1) < 0 \text{ as } \hat{l}_1 > \frac{l_1 + l_2}{2} \text{ and } l_1 > \hat{l}_1. \end{aligned}$$

Therefore, there exists unique solution $l_{20}^* \in (l_2, \frac{l_1 + l_2}{2})$ making $g(l_{20}^*) = 0$. When $y > \hat{l}_1 + \hat{l}_2$, $g(\hat{l}_2) < 0$ is equivalent to $l_{20}^* < \hat{l}_2 < y - \hat{l}_1$. This scenario corresponds to the first case in Corollary 1.

Scenario 2: The second scenario requires $y < \hat{l}_1 + \hat{l}_2$ and $g(\hat{l}_2) > 0$, where

$$g(\hat{l}_2) > 0 \Leftrightarrow y > 3\hat{l}_1 + 2l_2 - \hat{l}_2 - 2\frac{l_2\hat{l}_1}{\hat{l}_2}.$$

Therefore

$$\hat{l}_1 + \hat{l}_2 > y > 3\hat{l}_1 + 2l_2 - \hat{l}_2 - 2\frac{l_2\hat{l}_1}{\hat{l}_2} \rightarrow \hat{l}_1 + \hat{l}_2 > 3\hat{l}_1 + 2l_2 - \hat{l}_2 - 2\frac{l_2\hat{l}_1}{\hat{l}_2} \rightarrow \hat{l}_2 < l_2,$$

and scenario 2 has no-empty solution only if $\hat{l}_2 < l_2$. And we have following restrictions on the feasible region of \hat{l}_1 and \hat{l}_2 ,

$$y = l_1 + l_2 < \hat{l}_1 + \hat{l}_2, \hat{l}_2 < l_2 \Leftrightarrow \hat{l}_1 > l_1 + l_2 - \hat{l}_2 > l_1.$$

As $g(\hat{l}_2)$ is strictly convex over $\hat{l}_2 \in (0, l_2)$, and

$$\begin{aligned} g(\hat{l}_2 = 0) &= 2l_2\hat{l}_1 > 0 \\ g(\hat{l}_2 = l_2) &= l_2(l_1 - \hat{l}_1) < 0, \end{aligned}$$

we have the second case in Corollary 1. That is, there exists unique solution $l_{21}^* \in (0, l_2)$ making $g(l_{21}^*) = 0$. When $y < \hat{l}_1 + \hat{l}_2$, $g(\hat{l}_2) < 0$ is equivalent to $y - \hat{l}_1 < \hat{l}_2 < l_{21}^*$.

Additional Discussion for Scenario 1: Finally, while not mentioned in Corollary 1, we also briefly discuss the situation when $\hat{l}_1 \leq \frac{l_1 + l_2}{2}$ in Scenario 1. In this case, the feasible region of \hat{l}_2 becomes (l_2, \hat{l}_1) , with $g(\hat{l}_2 = \hat{l}_1) > 0$. Then the $g(\hat{l}_2) < 0$ has feasible solutions if and only if

$$\begin{cases} l_2 < \frac{3\hat{l}_1 + l_2 - l_1}{2} \\ \hat{l}_1 > \frac{3\hat{l}_1 + l_2 - l_1}{2} \\ g(\hat{l}_2 = \frac{3\hat{l}_1 + l_2 - l_1}{2}) < 0 \end{cases} \Leftrightarrow \begin{cases} \hat{l}_1 > \frac{l_1 + l_2}{3} \\ \hat{l}_1 < l_1 - l_2 \\ 9\hat{l}_1^2 - 2\hat{l}_1(3l_1 + l_2) + (l_2 - l_1)^2 > 0 \end{cases} \Leftrightarrow \begin{cases} l_1 \geq 3l_2 \\ \hat{l}_1 < \hat{l}_1 < \frac{l_1 + l_2}{2} \end{cases},$$

where $\hat{l}_1^* \in (\frac{l_1+l_2}{3}, \frac{l_1+l_2}{2})$ is the unique solution making $9\hat{l}_1^2 - 2\hat{l}_1(3l_1 + l_2) + (l_2 - l_1)^2 = 0$. As you expect, these inequalities mean strict restrictions. Under these conditions, there exists two distinct solutions l_{22}^* and l_{23}^* satisfying $l_2 < l_{22}^* < l_{23}^* < \frac{l_1+l_2}{2}$, $g(\hat{l}_2 = l_{22}^*) = 0$ and $g(\hat{l}_2 = l_{23}^*) = 0$. And both of the components improve with the weighted mechanism if and only if $l_{22}^* < \hat{l}_2 < l_{23}^*$.

Taking together, when $\hat{l}_1 \leq \frac{l_1+l_2}{2}$, the conditions for both the components improve are

$$\begin{cases} l_1 \geq 3l_2 \\ \frac{l_1+l_2}{3} < \hat{l}_1^* < \hat{l}_1 < \frac{l_1+l_2}{2} \\ l_2 < l_{22}^* < \hat{l}_2 < l_{23}^* < \frac{l_1+l_2}{2} \end{cases},$$

which are obviously quite strict. Therefore, we omit this situation and only focus on the cases with $\hat{l}_1 > \frac{l_1+l_2}{2}$ in the main text. \square

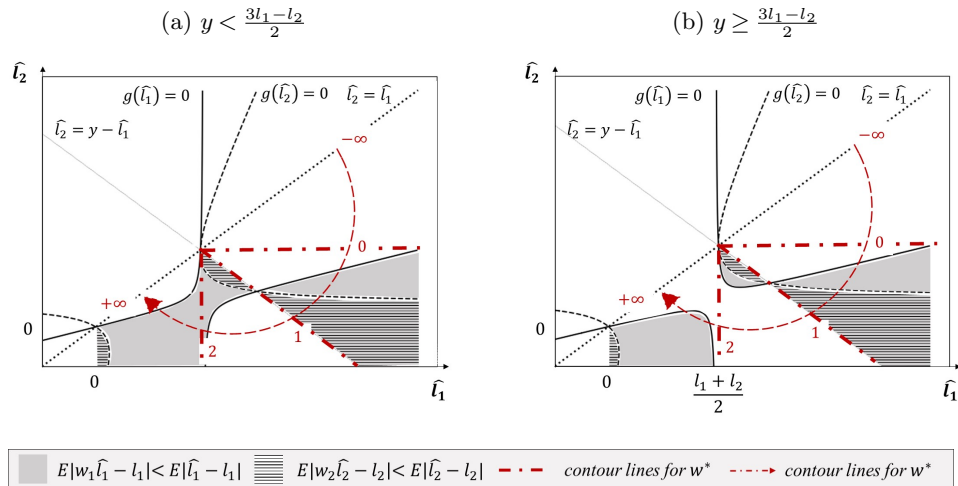
EC.1.6. Detailed Explanation of Observation 1

Following the definition of w^* when $N = 2$ (see Proposition 1),

$$w^* = \frac{y - 2\hat{l}_2}{\hat{l}_1 - \hat{l}_2} \Leftrightarrow \hat{l}_2 = \frac{w^*\hat{l}_1 - y}{w^* - 2} \text{ if } w^* \neq 2.$$

Mathematically, with given w^* , \hat{l}_2 is a linear function over \hat{l}_1 , making the contours for w^* in Figure 5 are straight lines with a fixed point $(\frac{l_1+l_2}{2}, \frac{l_1+l_2}{2})$. Specifically, when $w^* = 0, 1$ and 2 , the corresponding functions are $\hat{l}_2 = \frac{l_1+l_2}{2}$, $\hat{l}_2 = -\hat{l}_1 + l_1 + l_2$, and $\hat{l}_1 = \frac{l_1+l_2}{2}$, respectively. We draw the distribution of w^* in Figure EC.1, as a result, Observation 1 is quite intuitive.

Figure EC.1 Contours of w^* when $N = 2$



EC.2. Supplement Descriptions on Algorithms in Section 3.3

EC.2.1. Alternative Statistical Algorithms in Section 3.3.2

EC.2.1.1. MA and Weighted MA Suppose we want to forecast y_t at time t , and the time series data we use are $\mathbf{y} = \{y_{t-T}, \dots, y_{t-1}\}$. Then mathematically,

$$\begin{aligned} \text{For MA: } \hat{y}_t &= \frac{\sum_{j=1}^T y_{t-j}}{T}, \\ \text{For Weighted MA: } \hat{y}_t &= \frac{\sum_{j=1}^T \left(\frac{2(T-j+1)}{T(T-1)} y_{t-j} \right)}{T} = \frac{2 \sum_{j=1}^T ((T-j+1)y_{t-j})}{T^2(T-1)}. \end{aligned}$$

EC.2.1.2. Holt-Winters Additive Method (ETS) The holt-winters method decomposes the time series \mathbf{y} into the average (or baseline), trend, and seasonality components, denoted by \mathbf{l} , \mathbf{b} and \mathbf{s} , respectively. Suppose m is the frequency of seasonality, α , β and γ are pre-determined parameters between $[0, 1]$. Then in the additive ETS model, the prediction on time $t+h$ at time t is

$$\hat{y}_{t+h|t} = l_t + hb_t + s_{t+h-m \lfloor \frac{h-1}{m} + 1 \rfloor}$$

where $l_t = \alpha(y_t - s_{t-m}) + (1 - \alpha)(l_{t-1} + b_{t-1})$, $b_t = \beta(l_t - l_{t-1}) + (1 - \beta)b_{t-1}$, and $s_t = \gamma(y_t - l_{t-1} - b_{t-1}) + (1 - \gamma)s_{t-m}$.

EC.2.1.3. ARIMA Without and with Seasonality ARIMA is based on ARMA, an algorithm combining auto-regression and MA methods. Let p denote the order of the auto-regressive part, q denote the order of the moving average part, then the prediction \hat{y}_t of model $ARMA(p, q)$ follows

$$\hat{y}_t = \mu + \sum_{i=1}^p \phi_i \hat{y}_{t-i} + \sum_{j=1}^q \theta_j \varepsilon_{t-j} + \varepsilon_t,$$

where μ , ϕ_i and θ_j are the parameters to estimate according to the maximum likelihood principle, $\forall i \in \{1, \dots, p\}, j \in \{1, \dots, q\}$. When $\mathbf{y} = \{y_t\}$ is not stationary, the data need to be transformed by differencing d times, and the differenced time series \hat{y}'_t follows a similar form, i.e.,

$$\hat{y}'_t = \mu + \sum_{i=1}^p \phi_i \hat{y}'_{t-i} + \sum_{j=1}^q \theta_j \varepsilon_{t-j} + \varepsilon_t,$$

and is denoted by model $ARIMA(p, d, q)$ as \hat{y}_t is calculated by integration. If the time series also have significant seasonality, we need to make another differencing operation with the order D and lag (or seasonality frequency) m . The resulting seasonal ARIMA is denoted as $ARIMA(p, d, q)(P, D, Q)_m$, where P , D , and Q are the parameters of the seasonal part, corresponding to the lower case notation for the non-seasonal part.

EC.2.2. The FFORMA Algorithm

FFORMA is a hybrid algorithm for time series forecast proposed by Montero-Manso et al. (2020). Based on XGBoost, a gradient tree boosting model from Chen and Guestrin (2016), FFORMA combines a set of naive forecasting methods, such as the MA, ETS and ARIMA, to improve the forecasting accuracy. The training procedure is given in Table EC.1. Afterwards, based on the trained XGBoost model, the predictions are given by Eq. (5) in Section 3.3.2.

Table EC.1 Pseudocode for FFORMA Training (Montero-Manso et al. 2020)

Input:
$\{\mathbf{y}_1, \dots, \mathbf{y}_N\}$: N observed time series;
F : Set of functions for calculating features;
M : Set of naive forecasting methods.
<hr/>
<i>Data Preparation</i>
For $n = 1$ to N :
(a) Split \mathbf{y}_n into a training and test periods(sets);
(b) Calculate the set of features $f_n \in F$ over the training set;
(c) Fit every forecasting method $m \in M$ over the training set, and generate forecasts over the test set;
(d) Calculate forecast losses $L_m(f_n)$ with feature f_n and method m over the test set.
<i>Model Training</i>
Train an XGBoost model on $\mathbf{w} = \{w_m, \forall m \in M\}$ by minimizing $Loss = \sum_n \sum_m w_m(f_n) \times L_m(f_n)$.

EC.2.3. GBDT and XGBoost

Proposed by Friedman (2001), GBDT is a tree-based numerical heuristic. It consists of a series of sub-trees, in which each tree fits the residual between actual values and current predictions from previous trees. The final output is the addition of the outputs from subtrees. Specifically, let \mathbf{x} denote the input features, $\mathbf{y} = \{y_i, \forall i\}$ denote actual target values, and set $F_0(\mathbf{x}) = \text{average}(\mathbf{y})$, then the calculation procedure is an iterative process of

1. $\tilde{y}_i = y_i - F_{n-1}(\mathbf{x}_i), \forall i$;
2. $(\rho_n, \mathbf{a}_n) = \arg \min_{\rho, \mathbf{a}} \sum_i (\tilde{y}_i - \rho h(\mathbf{x}_i; \mathbf{a}))^2$;
3. $F_n(\mathbf{x}) = F_{n-1}(\mathbf{x}) + \rho_n h(\mathbf{x}; \mathbf{a})$;

until the termination condition is met, where $F_i(\mathbf{x})$ is the predictions after the m th iteration, and $\rho, h(\mathbf{x}; \mathbf{a}_m)$ are the parameters for the new sub-tree in the m th iteration.

The XGBoost algorithm is a specific case of GBDT. Specifically, when generating the sub-trees, XGBoost uses the Taylor expansion with first and second gradients to approximate the loss

function and further incorporate a regularization term penalizing the model complexity in the objective function. As a result, compared with classical GBDT, XGBoost shows better performance in accuracy and efficiency. We refer the readers to Chen and Guestrin (2016) for the fundamental mathematics and the operational details if interested.

EC.2.4. The STL Algorithm

As mentioned before, the STL algorithm is a classical decomposition algorithm proposed by Cleveland et al. (1990), and the detailed pseudocode is given in Table EC.2. In our case, we omit the component of residuals \mathbf{l}_R , and the forecasted value $\mathbf{l} = \mathbf{l}_T + \mathbf{l}_S$, where \mathbf{l}_T and \mathbf{l}_S are predicted by corresponding Loess algorithms.

Table EC.2 Pseudocode for STL Decomposition (Cleveland et al. 1990)

Input: time series data \mathbf{l}

Parameters:

- $n_{(p)}$: number of samples for a seasonality or period;
- $n_{(s)}, n_{(t)}, n_{(l)}$: parameters for corresponding Loess.

Definition: Subseries: the series within a period.

0. *Initialization:* $\mathbf{l}_T^{(0)} = 0, \boldsymbol{\delta}^{(0)} = 1$.

For $k = 0, 1, \dots, K$:

1. *Inner loop:*
 - (a) Detrending: Calculate $\mathbf{l} - \mathbf{l}_T^{(k)}$.
 - (b) Cycle-subseries smoothing: Use Loess with $q = n_{(s)}, d = 1, \delta = \boldsymbol{\delta}^{(k)}$ to regress the subseries; Get the temporary seasonal series $\mathbf{C}^{(k+1)}$, which is of length $N + 2n_{(p)}$ (from $-n_{(p)} + 1$ to $N + n_{(p)}$).
 - (c) Low-pass filtering:
 - (i) Calculate the moving average of $n_{(p)}$ on $\mathbf{C}^{(k+1)}$;
 - (ii) Calculate the moving average of 3 on the previous result from (i);
 - (iii) Use Loess with $q = n_{(l)}$ and $d = 1$ to regress the previous result from (ii);
 - (iv) Get the low-pass result $\mathbf{L}^{(k+1)}$, which is of size N (from time 1 to N).
 - (d) Detrending of smoothed cycle-subseries: Update $\mathbf{l}_S^{(k+1)} = \mathbf{C}^{(k+1)} - \mathbf{L}^{(k+1)}$.
 - (e) Deseasonalizing: Calculate $\mathbf{l} - \mathbf{l}_S^{(k+1)}$.
 - (f) Trend smoothing:
 - Use Loess with $q = n_{(t)}, d = 1$ and $\delta = \boldsymbol{\delta}^{(k)}$ to regress the previous result from (e), and get $\mathbf{l}_T^{(k+1)}$.
2. *Outer loop:*
 - Calculate $\mathbf{l}_R^{(k+1)} = \mathbf{l} - \mathbf{l}_T^{(k+1)} - \mathbf{l}_S^{(k+1)}$;
 - Calculate robustness weight $\boldsymbol{\delta}^{(k+1)} = B\left(\frac{|\mathbf{l}|}{\delta \text{median}(|\mathbf{l}|)}\right)$, where $B(u) = \begin{cases} (1 - u^2)^2 & \text{if } 0 \leq u < 1, \\ 0 & \text{if } u \geq 1. \end{cases}$.
3. *Repeat step 1 and 2 until* $k == K$ *or* $|\mathbf{l}_T^{(k)} - \mathbf{l}_T^{(k-1)}| + |\mathbf{l}_S^{(k)} - \mathbf{l}_S^{(k-1)}| \leq \varepsilon$.

EC.3. Supplementary Materials for Numerical Experiments

EC.3.1. Supplementary Details of Experiment Settings

Table EC.3 Features in the Practical Case of JD.com’s Sales Forecast

Stage	Model	Features
Stage 1: Preliminary decomposition	Baseline	Historical sales
	Promotion	X: Promotion types in sales history Y: Historical sales T: Prices in sales history W: Reference price, year, month, day, weekday
	Festival	Historical sales Festival level in sales history
Stage 2: ML improvement based on MQ-CNN	-	Historical Sales Time features: Year, month, day, weekday Product features: length of sales, product id, category, brand l: Decomposed predictions from stage 1

Table EC.4 Parameters in Numerical Experiments

Parameter	Description	Value	Experiment
T	Length of historical data	72	Practical
		60	Public
H	Forecasting horizon (days)	24	Practical
		30 or 31	Public
N	Number of preliminary decompositions	3	Practical
		2	Public
Learning rate	Learning rate in stage 2	1e-3	All
Batch size	Number of samples in each batch, include the features of 32 products, each with T samples	2304 (32*72)	Practical
		1920 (32*60)	Public
Number of batches (by sku)	Number of batches for each epoch	100	All
Epoch	Number of iterations in training	10-50	All
Repetition time	Number of repetitions of experiments	10	All
Units in the cell of Wavenet	Parameter of Wavenet	32	All
Number of hidden layers in Wavenet	Parameter of Wavenet	3	All
Units in MLP	Parameter of MLP	32	All
$n_{(p)}$	Seasonality parameter in STL	12	Public
$n_{(s)}, n_{(t)}, n_{(l)}$	Parameter for Loess in STL	1	Public

EC.3.2. Python Packages in Implementation**Table EC.5 Python Packages in Implementation**

Name	Description	Reference Link
statsmodels	Holt-Winters & ARIMA	https://pypi.org/project/statsmodels/
EconML	DML	https://github.com/microsoft/EconML
fforma	FFORMA	https://github.com/christophmark/fforma
STLDecompose	STL	https://github.com/jrmontag/STLDecompose
gluonts.model.wavenet	Wavenet	https://ts.gluon.ai/api/gluonts/gluonts.model.wavenet.html
gluonts.model.seq2seq	MQ-CNN	https://ts.gluon.ai/api/gluonts/gluonts.model.seq2seq.html
gluonts.model.deepar	DeepAR	https://ts.gluon.ai/api/gluonts/gluonts.model.deepar.html
gluonts.model.n_beats	N-BEATS	https://ts.gluon.ai/api/gluonts/gluonts.model.n_beats.html

EC.3.3. Supplementary Numerical Results**Table EC.6 Comparison on Model Performance by Month (Practical Data)**

Month	Algorithm	RMSE	P50_QL	Month	Algorithm	RMSE	P50_QL
Jun.	MQ-CNN	3.1469	0.2946	Aug.	MQ-CNN	1.9988	0.1989
Jun.	Preliminary Decomposition I <i>(Additive Combination)</i>	2.9050	0.2452	Aug.	Preliminary Decomposition I <i>(Additive Combination)</i>	1.9799	0.1960
Jun.	Preliminary Decomposition II <i>(Simple MLP Combination)</i>	3.0391	0.2829	Aug.	Preliminary Decomposition II <i>(Simple MLP Combination)</i>	1.9205	0.1885
Jun.	W-R Algorithm ($\alpha = 1$)	2.2872	0.2213	Aug.	W-R Algorithm ($\alpha = 1$)	1.8987	0.1830
Jun.	DeepAR	3.3236	0.3281	Aug.	DeepAR	2.3000	0.2648
Jun.	N-BEATS	3.4232	0.3632	Aug.	N-BEATS	2.3143	0.2776
Jul.	MQ-CNN	2.4616	0.2106	Sep.	MQ-CNN	2.4356	0.2255
Jul.	Preliminary Decomposition I <i>(Additive Combination)</i>	2.4021	0.2134	Sep.	Preliminary Decomposition I <i>(Additive Combination)</i>	2.3547	0.2227
Jul.	Preliminary Decomposition II <i>(Simple MLP Combination)</i>	2.3633	0.2015	Sep.	Preliminary Decomposition II <i>(Simple MLP Combination)</i>	2.1745	0.2111
Jul.	W-R Algorithm ($\alpha = 1$)	1.8987	0.1954	Sep.	W-R Algorithm ($\alpha = 1$)	2.0738	0.2009
Jul.	DeepAR	2.4727	0.2252	Sep.	DeepAR	2.4374	0.2260
Jul.	N-BEATS	2.5023	0.2410	Sep.	N-BEATS	2.7691	0.3250